AMERICAN SOCIETY FOR MICROBIOLOGY | Infection and Immunity

Shiga Toxins Activate the NLRP3 Inflammasome Pathway To Promote Both Production of the Proinflammatory Cytokine Interleukin-1β and Apoptotic Cell Death

Moo-Seung Lee,[a] Haenaem Kwon,[a] Eun-Young Lee,[a] Dong-Jae Kim,[b] Jong-Hwan Park,[c] Vernon L. Tesh,[d] Tae-Kwang Oh,[a] Myung Hee Kim[a]

Infection and Immunity Research Center, Korea Research Institute of Bioscience and Biotechnology, Daejeon, South Korea[a]; Division of Drug Screening and Evaluation, New Drug Development Center, Osong Medical Innovation Foundation, Cheongju, Chungbuk, South Korea[b]; College of Veterinary Medicine, Chonnam National University, Gwangju, South Korea[c]; Department of Microbial Pathogenesis and Immunology, Texas A&M University Health Science Center, Bryan, Texas, USA[d]

Shiga toxin (Stx)-mediated immune responses, including the production of the proinflammatory cytokines tumor necrosis-α (TNF-α) and interleukin-1β (IL-1β), may exacerbate vascular damage and accelerate lethality. However, the immune signaling pathway activated in response to Stx is not well understood. Here, we demonstrate that enzymatically active Stx, which leads to ribotoxic stress, triggers NLRP3 inflammasome-dependent caspase-1 activation and IL-1β secretion in differentiated macrophage-like THP-1 (D-THP-1) cells. The treatment of cells with a chemical inhibitor of glycosphingolipid biosynthesis, which suppresses the expression of the Stx receptor globotriaosylceramide and subsequent endocytosis of the toxin, substantially blocked activation of the NLRP3 inflammasome and processing of caspase-1 and IL-1β. Processing and release of both caspase-1 and IL-1β were significantly reduced or abolished in Stx-intoxicated D-THP-1 cells in which the expression of NLRP3 or ASC was stably knocked down. Furthermore, Stx mediated the activation of caspases involved in apoptosis in an NLRP3- or ASC-dependent manner. In Stx-intoxicated cells, the NLRP3 inflammasome triggered the activation of caspase-8/3, leading to the initiation of apoptosis, in addition to caspase-1-dependent pyroptotic cell death. Taken together, these results suggest that Stxs trigger the NLRP3 inflammasome pathway to release proinflammatory IL-1β as well as to promote apoptotic cell death.

Shiga toxins (Stxs) are a family of genetically, structurally, and functionally related bacterial protein toxins expressed by the enteric pathogens *Shigella dysenteriae* serotype 1 and Stx-producing *Escherichia coli* (STEC). These toxins are the primary virulence factors associated with bloody diarrhea, which may progress to life-threatening systemic sequelae such as acute renal failure syndrome, also known as hemolytic uremic syndrome (HUS), and central nervous system abnormalities (1).

Based on antigenic similarity to the prototypical Stx expressed by *S. dysenteriae* serotype 1, STEC expresses two related Stxs. Stx type 1 (Stx1) is essentially identical to Stx, whereas Stx type 2 (Stx2) is only 56% identical to Stx/Stx1 at the amino acid level (2, 3). Epidemiological studies and clinical observations showed that infections with Stx2-producing strains of STEC are more likely to cause serious extraintestinal complications (4, 5).

Structural studies of Stxs reveal that all of these toxins are composed of a monomeric A subunit noncovalently associated with a homopentameric ring of B subunits (6, 7). The A subunit inhibits protein synthesis by its RNA *N*-glycosidase activity, whereas the B subunits bind the neutral membrane glycolipid globotriaosylceramide (Gb3) on the surface of susceptible host cells (8). Following endocytosis, the toxin is transported in a retrograde manner, via the *trans*-Golgi network and Golgi apparatus, to the lumen of the endoplasmic reticulum (ER) (9). During retrotranslocation, the A subunit is proteolytically processed to produce the enzymatically active A1 fragment (10–14). Translocation of the A1 fragment into the cytosol is required for cleavage of a single adenine residue (at position A4324 in rat) located in the α-sarcin/ricin loop within the 28S rRNA component of eukaryotic ribosomes (12, 15). This site-specific rRNA depurination reaction results in the inhibition of protein synthesis.

Multiple signaling cascades are activated in host cells in response to protein synthesis inhibitors that modify the 3′ end of the 28S rRNA component of the eukaryotic ribosome, including the ribotoxic stress response that activates the c-Jun N-terminal (JNK) mitogen-activated protein kinase (MAPK) signaling pathway (16). In particular, Stx-mediated ribotoxic stress induces apoptosis or programmed cell death in various cell types (17). Stxs also activate the ER stress response, which is normally triggered by the accumulation of misfolded proteins within the ER (18). Prolonged activation of ER stress is associated with the induction of apoptosis (18, 19). Although the stress responses activated by Stxs appear to be cell type specific, the maturation state of a given cell may determine its cellular response to intoxication. For example, Stx treatment of undifferentiated (monocytic) THP-1 cells (UD-THP-1) leads to rapid apoptosis, whereas intoxication of differentiated (macrophage-like) THP-1 cells (D-THP-1) results in the activation of both apoptotic and survival signaling pathways (20, 21).

Many studies have shown that Stxs elicit a proinflammatory

Received 25 August 2015 **Returned for modification** 18 September 2015
Accepted 16 October 2015

Accepted manuscript posted online 26 October 2015

Citation Lee M-S, Kwon H, Lee E-Y, Kim D-J, Park J-H, Tesh VL, Oh T-K, Kim MH. 2016. Shiga toxins activate the NLRP3 inflammasome pathway to promote both production of the proinflammatory cytokine interleukin-1β and apoptotic cell death. Infect Immun 84:172–186. doi:10.1128/IAI.01095-15.

Editor: B. A. McCormick

Address correspondence to Myung Hee Kim, mhk8n@kribb.re.kr.

response, including the elevated production of TNF-α, macrophage inflammatory protein 1 (MIP-1), IL-1β, IL-8, IL-6, growth-related oncogene α (Groα), and Groβ, both *in vitro* and *in vivo* (22). The orchestrated induction of cytokine and chemokine expression is essential to limit pathogen dissemination and initiate wound healing (23). Following ingestion of toxin-producing bacteria, Stxs produced in the gut are transferred across the polarized human intestinal epithelial cell monolayer into the circulating blood. Stxs are thought to directly damage vascular endothelial cells, leading to localized inflammation. Thus, Stxs may elicit proinflammatory cytokine expression in neutrophil- and macrophage-rich microenvironments (24). In human macrophage-like THP-1 cells, Stxs regulate cytokine levels through the transcription factors NF-κB, Egr-1, and ATF-3, as well as through activation of MAPK cascades (25, 26). Stx1-induced activation of the phosphatidylinositol 3-kinase (PI3K)-Akt-mTOR pathway mediates a transient increase in proinflammatory cytokine level, which in turn results in the hyperphosphorylation of the translation initiation factor 4E-BP and inactivation (by phosphorylation) of the positive cytokine regulatory factor glycogen synthase kinase 3 (GSK-3) (27). Finally, Stxs induce the expression of dual-specificity phosphatases (DUSPs), also called MAP kinase phosphatases, which negatively regulate MAPK activation, suggesting that the activation of cytokine signaling by Stxs ultimately downregulates the proinflammatory cytokine expression (28).

Crucial to the activation of caspase-1 and processing of the proinflammatory cytokine IL-1β is the formation of a multiprotein complex termed the inflammasome (29, 30). Despite recent progress in understanding how Stxs induce proinflammatory cytokines, the involvement of inflammasomes in Stx-induced cytokine expression and their role in disease progression remain incompletely understood. Recent studies showed that the ribosome-inactivating protein ricin activates inflammasomes containing the nucleotide-binding domain and leucine-rich repeat containing receptor (NLR) protein 3 (NLRP3). Inflammasome activation is associated with the cleavage of procaspase-1 into the p10 and p20 subunits of active caspase-1, as well as the processing and secretion of the active form of IL-1β (31). However, the mechanism by which Stx1 or Stx2 regulates the production of proinflammatory cytokines, including IL-1β, has not been elucidated. Here, we report that receptor Gb3-dependent Stx endocytosis activates NLRP3 inflammasome signaling to trigger the production of proinflammatory cytokine IL-1β, as well as to promote caspase-8/3-dependent apoptosis, in the toxin-sensitive macrophage-like THP-1 cell line.

MATERIALS AND METHODS

Antibodies and reagents. Mouse monoclonal antibody against actin and rabbit monoclonal antibodies against IL-1β, caspase-1, caspase-3, caspase-8, NLRP3, and apoptosis-associated speck-like protein containing CARD (ASC) were purchased from Cell Signaling Technology (Danvers, MA). Mouse monoclonal antibody specific for CD77/Gb3 was purchased from LifeSpan Bioscience (Seattle, WA). Phorbol 12-myristate 13-acetate (PMA) and lipopolysaccharides (LPS) were purchased from Sigma-Aldrich (St. Louis, MO). The glucosylceramide synthetase inhibitor DL-*threo*-1-phenyl-2-decanoylamino-3-morpholino-1-propanol (D-*threo*-PDMP) was acquired from Matreya LLC (Pleasant Gap, PA). For short interfering RNA (siRNA) transfection, TransIT-TKO transfection reagent was obtained from Mirus Bio (Madison, WI).

Toxins. Stx1 was purified as previously described (4, 5). Toxin was passed through ActiClean Etox columns (Sterogene Bioseparations, Carlsbad, CA) to remove trace endotoxin contaminants; samples treated in this manner contained <0.1 ng/ml endotoxin as determined by the *Limulus* amebocyte lysate assay (Associates of Cape Cod, East Falmouth, MA). Purified Stx1 holotoxin containing a double mutation (E167Q and R170L) in the A subunit (StxA1$^-$), which dramatically reduces enzymatic activity, was a kind gift of Shinji Yamasaki, Osaka Prefecture University, Osaka, Japan (32). Recombinant purified Stx2, StxA2$^-$ toxoid (Y77S/E167Q/R170L), and StxB2 subunits were obtained from NIAID, NIH Biodefense and Emerging Infections Research Repository (BEI Resources, Manassas, VA).

Cell culture and differentiation. All cells used in this study were maintained at 37°C in a 5% CO_2-95% air atmosphere in a humidified incubator. The human myelogenous leukemia cell line THP-1 (TIB-202; American Type Culture Collection, Manassas, VA) was cultured in RPMI 1640 medium containing 10% fetal bovine serum (FBS; Gibco-BRL, Grand Island, NY), penicillin (100 U/ml), and streptomycin (100 μg/ml). Cells maintained under these conditions were considered to be undifferentiated, monocytic THP-1 cells (UD-THP-1). THP-1-defNLRP3 cells (in which the level of NLRP3 was stably knocked down) or THP-1-defASC cells (in which the level of ASC was stably knocked down) were obtained from InvivoGen (San Diego, CA). UD-THP-1 cells (1.0×10^6 cells/ml) were differentiated to the adherent macrophage-like state by treatment with 50 ng ml^{-1} PMA for 36 h. Plastic-adherent cells were washed three times with fresh medium lacking PMA but containing 10% FBS, penicillin (100 U/ml), and streptomycin (100 μg/ml). The medium was changed every 24 h for the next 3 days. The resultant cells were considered differentiated, macrophage-like THP-1 cells (D-THP-1). Experiments were performed on or after the fourth day following PMA removal. CD14$^+$ primary human monocytes were obtained from Lifeline Cell Technology (Carlsbad, CA). Primary human monocytes were cultured in 6-well tissue culture plates (Thermo Fisher Scientific, Waltham, MA) in RPMI 1640 medium containing 10% human serum (Thermo Fisher Scientific). Culture of human monocyte-derived macrophages (hMDM) was performed as previously described (33). The medium was replaced every 3 days, and adherent cells were used for experiments within 11 days of plating. Human T84 colon carcinoma cells were purchased from the European Collection of Cell Cultures (Salisbury, United Kingdom). Cells were cultured in Dulbecco's modified Eagle's medium (DMEM)–F-12 (1:1) supplemented with 10% FBS.

Preparation of cellular lysates and Western blotting. Twelve hours prior to stimulation, D-THP-1 cells (5×10^6 cells per well) were serum starved in RPMI 1640 medium containing 0.5% FBS to reduce background kinase signaling. Cells were treated for 0 to 24 h with Stx1 (400 ng/ml), Stx2 (10 ng/ml), StxA1$^-$ (400 ng/ml), StxA2$^-$ (10 ng/ml), or StxB2 (10 ng/ml). Cells were harvested and lysed at 4°C in modified radioimmunoprecipitation assay buffer (0.5% Nonidet P-40, 1.0% sodium deoxycholate, 150 mM NaCl, 50 mM Tris-HCl [pH 7.5], 0.25 mM sodium pyrophosphate, 2 mM sodium vanadate, 2 mM sodium fluoride, 10 μg/ml aprotinin, 1.0 μg/ml leupeptin, 1.0 μg/ml pepstatin, and 0.2 mM phenylmethylsulfonyl fluoride [PMSF]) supplemented with protease inhibitor (GenDEPOT, Barker, TX) and phosphatase inhibitor (GenDEPOT). For detection of caspase-1, cells were lysed with 3-[(3-cholamidopropyl)-dimethylammonio]-1-propanesulfonate (CHAPS) modified lysis buffer [50 mM piperazine-*N*,*N*′-bis(2-ethanesulfonic acid)–HCl (pH 6.5), 2 mM EDTA, 0.1% CHAPS, 20 μg/ml leupeptin, 10 μg/ml pepstatin A, 10 μg/ml aprotinin, 5 mM dithiothreitol (DTT), and 1 mM PMSF] supplemented with protease and phosphatase inhibitors. Extracts were collected and cleared by centrifugation at 15,000 × *g* for 20 min. Cell lysates were prepared as previously described (18, 33). Protein concentrations of each extract were determined using the DC protein assay (Bio-Rad, Hercules, CA). Equal amounts of proteins (50 to 80 μg per lane) were separated by SDS-PAGE on 4 to 12% Bis-Tris Plus gels (Life Technologies, Grand Island, NY) in morpholineethanesulfonic acid (MES)-SDS running buffer

(Life Technologies) and transferred to nitrocellulose or polyvinylidene difluoride (PVDF) membranes. The membranes were washed with TBST wash buffer (20 mM Tris-HCl [pH 7.6], 137 mM NaCl, and 0.1% Tween 20) and blocked with casein (3 to 5%) dissolved in 50 mM Tris-HCl (pH 7.6), 150 mM NaCl, and 0.1% Tween 20. The membranes then were incubated with primary antibodies at 4°C for 24 h. After washing, the membranes were incubated with horseradish peroxidase-labeled secondary antibodies at room temperature for 1 h. Bands were visualized using the Western Lightning chemiluminescence system on an Image Quant LAS 4000 (GE Healthcare). The data shown are representative of at least three independent experiments. Relative protein levels were determined using the NIH ImageJ software.

Knockdown assay. Specific SMARTpool siRNAs targeting NLRP3, ASC, NLRC4, caspase-1, and AIM2 and nontargeting negative-control siRNA were purchased from GE Healthcare Dharmacon, Inc. (Pittsburgh, PA). Macrophage-like THP-1 cells were transfected with each siRNA (400 pmol) using the *Trans*IT-TKO transfection reagent. Forty-eight hours after transfection, the medium was removed, the cells were washed three times with PBS, and the medium was replaced with RPMI 1640 supplemented with 0.5% FBS. For studies using THP-1 cells with stable knockdown of NLRP3 inflammasome function, THP-1-defNLRP3 or THP-1-defASC cells were treated with PMA to generate differentiated cells with reduced NLRP3 activity (D-THP-1^{NLRP3KD}) or reduced ASC activity (D-THP-1^{ASCKD}), respectively. Subsequently, siRNA-transfected D-THP-1 cells, D-THP-1^{NLRP3KD} or D-THP-1^{ASCKD}, were incubated with Stx1 (400 ng/ml) or Stx2 (10 ng/ml) for 0 to 24 h. Cell lysates were prepared, and Western blotting was performed with specific antibodies against caspase-1, IL-1β, caspase-3, caspase-8, or β-actin. To address the influence of silencing of NLRP3, ASC, caspase-1, NLRC4, or AIM2 on inflammasome-mediated cytokine production, supernatants were collected for measurement of soluble cytokines by enzyme-linked immunosorbent assay (ELISA).

Quantitative RT-PCR analysis. Following toxin treatment, total RNA was isolated from cells using the RNAqueous kit (Life Technologies, Grand Island, NY), a phenol-free, filter-based RNA isolation system. The resultant samples were treated with RNase-free DNase at 37°C for 30 min to remove genomic DNA contamination, followed by heat inactivation at 95°C for 20 min. Levels of target genes were measured by reverse transcription-PCR (RT-PCR) using the following primers: *NLRP3*, 5′-TGATGTTCTGTGAAGTGCTGAA-3′ (forward) and 5′-CGCACTTTTTGTCTCATAATTAG-3′ (reverse); *ASC*, 5′-AGTTCAAGCTGAAGCTGCTGT-3′ (forward) and 5′-CCAGCTTGTCGG TGAGGT-3 (reverse); and *Actin*, 5′-CCTGGCACCCAGCACAAT-3′ (forward) and 5′-GCCGATCCACACGGAGTACT-3′ (reverse). All PCR primers for target genes were designed using the Roche Assay Design Center (http://www.universalprobelibrary.com) and synthesized at Bioneer (Daejeon, South Korea). Quantitative RT-PCR assays were carried out in a LightCycler 96 (Roche Diagnostics, Mannheim, Germany) using RealHelix quantitative PCR (qPCR) kits (Nanohelix, Daejeon, South Korea). Ten nanograms of total RNA was used in reverse transcription reactions. The PCR program was cDNA synthesis at 50°C for 40 min; initial denaturation at 95°C for 12 min; 40 cycles of denaturation at 95°C for 20 s, annealing at 50°C for 30 s, and extension at 60°C for 1 min; and a final extension at 60°C for 10 min. Raw fluorescence data were normalized against the corresponding level of *GAPDH* mRNA. Relative expression values were calculated using LightCycler 96 software, version 1.01.

Detection of ASC oligomerization. For analysis of ASC oligomerization, D-THP-1 cells were treated with Stx1, Stx2, or LPS for 1 to 4 h. Cells were harvested using CHAPS lysis buffer and centrifuged at 6,000 rpm at 4°C for 15 min. The resultant pellet fractions were collected and resuspended in PBS, cross-linked with disuccinimidyl suberate (DSS), and mixed with native gel loading buffer (Bio-Rad). Samples were separated on Mini-PROTEAN TGX precast native gels (Bio-Rad) and analyzed by Western blotting with anti-ASC antibody.

Cytotoxicity assay. D-THP-1 cells (1.0×10^4 cells per well) were seeded in 96-well microtiter plates prior to treatment with Stx1 (0 to 400 ng/ml) for 0 to 24 h in RPMI 1640 medium containing 0.5% FBS. Cytotoxicity was determined by a colorimetric assay (34) using 3-(4,5-dimethylthiazol-2-yl)-5-(carboxymethoxyphenyl)-2-(4-sulfophenyl)-2H-tetrazolium, inert salt (MTS) (Promega, Madison, WI). MTS (50 μl) was added to each well, and incubation continued at 37°C for 2 h in a 5% CO_2 humidified incubator. Optical density at 490 nm was recorded using an automated microtiter plate reader (Biotek, Winooski, VT). The percentage of cell death was determined using the following equation: percentage of cell death = [(average OD_{490} of treated cells − average OD_{490} of control cells)/(average OD_{490} of control cells)] × 100, where OD_{490} is the optical density at 490 nm. Background absorbance at 630 nm, measured in untreated cells, was subtracted from each sample reading. The reference wavelength of 630 nm was used to subtract background contributed by excess cell debris and other nonspecific absorbance.

Caspase-3/7 activity assay. D-THP-1 cells in 96-well microtiter plates were treated with Stx1 for 12 h in RPMI 1640 medium containing 0.5% FBS. Caspase-3/7 was detected using the Caspase-Glo 3/7 assay kit (Promega, Madison, WI). Glo reagent (100 μl) was added to each well and incubated for 0.5 to 3 h in a 5% CO_2 humidified incubator. Luminescence was detected on a GloMax 96 microplate luminometer (Promega).

ELISA. Accumulated cytokines were determined using caspase-1, IL-1β, IL-8, or Groα ELISA kits purchased from R&D Systems (Minneapolis, MN). D-THP-1 was incubated in starvation media for 4 to 12 h prior to Stx treatment. Stimulated D-THP-1 cell culture media were collected after centrifugation at 14,000 × *g* for 20 min at 4°C. Collected media were concentrated using Amicon ultracentrifugal filter systems (EMD Millipore, Billerica, MA). Concentrated supernatant samples were added to 96-well polystyrene microtiter plates coated with anti-IL-8, anti-IL-1β, or anti-Groα.

TUNEL assay. The apoptosis of adherent macrophage-like D-THP-1 cells and cells in which ASC or NLRP3 expression was stably knocked down was determined using an *in situ* cell death detection kit (Roche, Mannheim, Germany). Briefly, cells (2.0×10^5 cells per well) were differentiated on 8-well Lab-Tek chamber slides (Thermo Scientific), resulting in approximately 1.0×10^5 viable cells per well. Cells were left untreated or were treated with Stx1 (400 ng/ml) for 24 h and then fixed in freshly prepared 4% paraformaldehyde for 1 h, rinsed with PBS, and treated with permeabilization solution for 2 min on ice. Following washing, terminal deoxynucleotidyltransferase-mediated dUTP-biotin nick end labeling (TUNEL) reaction mix was added, the samples were incubated for 1 h at 37°C in the dark, and the cells again were washed in PBS. To count TUNEL-positive cells, the total number of TUNEL-positive cells was determined from 15 different fields (magnification, ×20) for each treatment condition in three independent experiments. In parallel, total cell numbers were determined by counting Hoechst 33342 (Thermo Scientific Inc.)-stained nuclei in samples from each treatment condition. Percentages of TUNEL-positive cells (above the value in untreated controls) were calculated with the following equation: percentage apoptosis = (number of TUNEL-positive cells/total number of Hoechst 33342 − positive total cells) × 100.

Statistics. Data are reported as means ± standard errors of the means (SEM) from at least three independent experiments. Statistical analyses of data were performed using GraphPad Prism software (GraphPad, San Diego, CA). Depending on the assay, $P < 0.001$ or $P < 0.01$ was considered significant.

RESULTS

Shiga toxin targets the NLRP3 inflammasome pathway. A multiprotein complex called the inflammasome, consisting of NLRP3 and the adaptor protein ASC, forms in response to multiple damage-inducing agents, including bacterial pathogens and metabolic danger signals. The inflammasome activates caspase-1 to process pro-IL-1β, resulting in the production of the highly

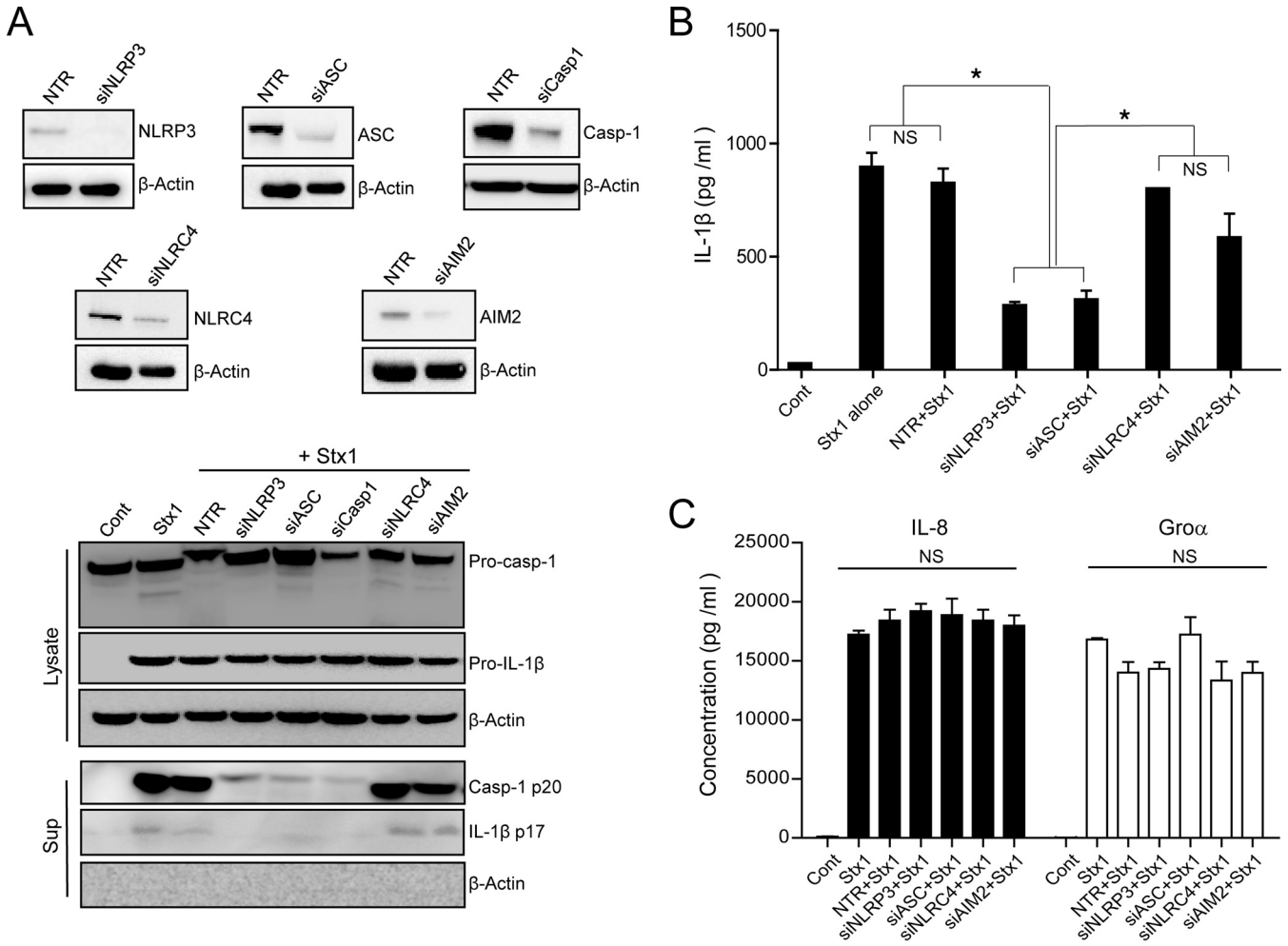

FIG 1 Shiga toxin targets the NLRP3 inflammasome pathway. (A) D-THP-1 cells were transfected for 60 h with siRNAs targeting NLRP3 (siNLRP3), ASC (siASC), caspase-1 (siCasp1), NLRC4 (siNLRC4), or AIM2 (siAIM2) or with nontargeting siRNA (NTR). After washing, cell lysates were collected and the knockdown of proteins was confirmed by Western blotting. (Upper) β-Actin was used as a control for equal protein loading. (Lower) Knockdown cells exposed to Stx1 (400 ng/ml) for 12 h were evaluated for Casp-1 p20 or IL-1β release into the media. β-Actin was used as a control for equal protein loading. (B and C) Effect of knockdown of NLRP3 (siNLRP3), ASC (siASC), NLRC4 (siNLRC4), and AIM2 (siAIM2) on the release of IL-1β, IL-8, and Groα into media collected from D-THP-1 cells treated with Stx1 for 24 h. Cont, untreated control; Pro-casp-1, procaspase-1; Casp-1 p20, active form of p20 subunit of caspase-1; Pro-IL-1β, unprocessed pro-form of IL-1β; IL-1β p17, active form of proteolytically processed IL-1β; Sup, supernatant. Results are means ± SEM from two experiments, each performed in triplicate. Asterisks indicate a statistically significant difference in IL-1β level ($P < 0.001$). NS, not significant.

proinflammatory molecule IL-1β (35–37). Although previous studies reported that the formation of the NLRP3 inflammasome is required for processing and release of IL-1β in bone marrow-derived macrophages treated with a panel of well-characterized protein synthesis inhibitors (31, 38), the mechanism underlying the proinflammatory response to Shiga toxin has not yet been studied.

To address this issue, we first evaluated the composition of the inflammasome formed in response to Stx1 in D-THP-1 cells by siRNA-induced knockdown of the following genes: NLRP3, NLR family CARD domain-containing protein 4 (NLRC4), absent in melanoma 2 (AIM2), ASC, and caspase-1. Stx1-mediated caspase-1 activation and IL-1β processing were significantly impaired in cells transfected with NLRP3-, ASC-, or caspase-1-specific siRNA but not in cells transfected with NLRC4- or AIM2-specific siRNA or nontargeting negative-control siRNA (Fig. 1A), indicating that Stx1 targets the NLRP3 inflammasome for caspase-1 activation in D-THP-1 cells. The best-characterized pathway leading to the secretion of immunoreactive IL-1β involves the inflammasome-mediated activation of caspase-1 (35, 39, 40). Therefore, we further examined the effect of NLRP3, NLRC4, AIM2, or ASC knockdown on the production of mature IL-1β, IL-8, and Groα after 24 h of exposure to Stx1. Stx1 treatment of D-THP-1 cells transfected with nontargeting siRNA (NTR), siNLRC4, or siAIM2 or not transfected with any siRNA produced significantly higher levels of IL-1β than cells not treated with the toxin (Fig. 1B). In contrast, siNLRP3- or siASC-transfected cells treated with Stx1 produced significantly lower levels of IL-1β (Fig. 1B), demonstrating that the inflammatory response to the toxin is dependent on the NLRP3 inflammasome. Several studies have shown that Stxs stimulate the production of proinflammatory factors other than IL-1β, including TNF-α, MIP-1, IL-8, IL-6, and Groα (22). Therefore, we investigated whether inflammasome components affect the Stx1-induced production of additional proinflamma-

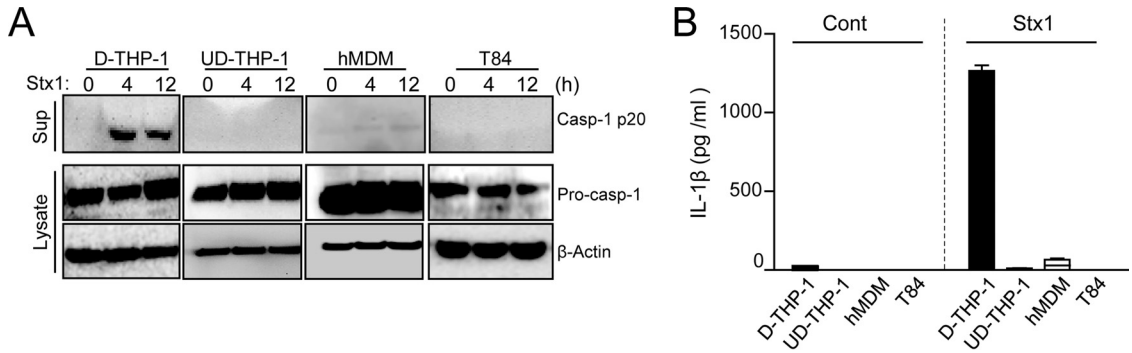

FIG 2 Stx1 triggers caspase-1-dependent IL-1β release only in differentiated macrophage-like cells. (A) Casp-1 p20 levels were elevated only in Stx1-treated D-THP-1 cells. Western blotting was used to measure levels of activated caspase-1 (Casp-1 p20), procaspase-1 (Pro-casp-1), and β-actin in media or lysates prepared from toxin-sensitive D-THP-1 and UD-THP-1 cells, toxin-resistant human primary monocyte-derived macrophages (hMDM), and toxin receptor Gb3-deficient T84 cells stimulated with Stx1 (400 ng/ml) for 4 or 12 h. D-THP-1, UD-THP-1, hMDM, and T84 cells were stimulated with Stx1 (400 ng/ml) for 24 h. (B) Levels of soluble IL-1β released from various cell types treated with Stx1. The quantitation of IL-1β was performed by ELISA. Mean cytokine values (pg/ml) from two independent experiments were calculated and are expressed as means ± SEM.

tory factors. Regardless of the expression status of inflammasome components, the chemokines IL-8 and Groα were released into the media at comparable levels (Fig. 1C).

Stx promotes caspase-1-dependent IL-1β release only in toxin-sensitive differentiated macrophage-like cells. Stxs trigger signaling pathways in a cell type-specific manner; consequently, Stx treatment leads to terminal executioner caspase-8/3 activation only in toxin-sensitive THP-1 or HK-2 cells, but not in toxin-refractory primary human monocyte-derived macrophages (hMDM) (33). To determine whether inflammasome activation is critical for the susceptibility of host cells to the cytotoxic activity of Stxs, we investigated the ability of toxins to produce active Casp-1 p20 and mature IL-1β in both toxin-sensitive (D-THP-1 and UD-THP-1 cells) and toxin-resistant cell types (hMDM and T84 epithelial cells). Only D-THP-1 cells exhibited caspase-1 activation upon toxin stimulation, whereas UD-THP-1 cells, which are not capable of producing cytokines following toxin treatment, as well as the highly toxin-refractory hMDM and T84 cells, did not convert procaspase-1 to the active form (Fig. 2A). The levels of Casp-1 p20 released from Stx1-intoxicated D-THP-1 cells were significantly elevated after 4 and 12 h, respectively, relative to those from untreated cells (0 h). However, Casp-1 p20 was not secreted at detectable levels from Stx1-treated UD-THP-1, hMDM, and T84 cells.

To assess whether the caspase-1 activation is correlated with the processing of inactive pro-IL-1β into mature IL-1β, we analyzed supernatants collected from the Stx1-treated cells by Western blotting and ELISA. Stx1 treatment induced pro-IL-1β processing and extracellular release of IL-1β only in D-THP-1 cells (Fig. 2B). These results suggest that Stx1 prompts caspase-1-dependent IL-1β release and induces caspase-8/3 activation, which leads to apoptotic cell death, in toxin-sensitive differentiated macrophage-like THP-1 cells (see below).

Stxs activate NLRP3 inflammasome-mediated caspase-1-dependent IL-1β secretion by promoting oligomerization of ASC. Previous studies focused on the Stx-induced intracellular signaling pathways leading to the activation of innate immunity, particularly cytokine and chemokine expression. Those studies showed that Stx treatment of primary human monocyte-derived macrophages and D-THP-1 cells induces TNF-α and IL-1β expression (41, 42). Because our results demonstrated that Stx targets the NLRP3 inflammasome pathway, we further characterized the effect of Stxs on inflammasome function in relation to processing of IL-1β. To monitor the presence of caspase-1 p20 subunit (Casp-1 p20) as a direct readout of inflammasome function, D-THP-1 cells first were primed with LPS or left unprimed, followed by treatment with 400 ng ml^{-1} of Stx1 for 1 to 12 h. LPS, a well-characterized activator of inflammasome function (43, 44), was used to assess additive effects on caspase-1 activation. In a mouse model of HUS, both LPS and Stxs are required to initiate thrombotic microangiopathy (45). Therefore, it is reasonable to speculate that synergistic effects of Stxs and LPS contribute to the activation of the inflammasome in macrophage-like cells. Stx1 treatment with or without LPS induced inflammasome function and increased active Casp-1 p20 levels in cell lysates (Fig. 3A). Activation of inflammasome function occurred rapidly in response to all treatments, with Casp-1 p20 reaching maximal levels at 4 h after treatment. Substantial levels of caspase-1 activation occurred at 4 h in cells cotreated with Stx1 and LPS. Consistent with earlier studies (41), UD-THP-1 cells treated with Stx1 alone did not produce pro-IL-1β (Fig. 3A). In addition, we monitored supernatants collected from cells treated with Stx1 or Stx2 for the presence of Casp-1 p20, a well-accepted means of monitoring inflammasome activation (46) (Fig. 3B). Western blotting revealed the appearance of the active form of caspase-1 in supernatants collected from toxin-treated cells (Fig. 3B, upper). In addition, we measured the amounts of secreted active caspase-1 induced by Stx1 or Stx2 by ELISA of culture supernatants. Levels of active Casp-1 p20 were remarkably increased in supernatants collected from D-THP-1 cells treated with Stx1 or Stx2 relative to those from untreated cells (Fig. 3B, lower).

To further explore inflammasome activation, we performed the inflammasome adaptor ASC oligomerization assay, which measures the amount of oligomeric ASC (pyroptosomes) in the Nonidet P-40-insoluble low-speed pellets of stimulated cells (46, 47). ACS in Stx-treated cells was oligomerized regardless of the presence of LPS (Fig. 3C). Together, these data suggest that Stxs stimulate inflammasome function via oligomerization of the adaptor protein ASC, a critical step in caspase-1 activation, extracellular release of IL-1β, and pyroptotic cell death (39).

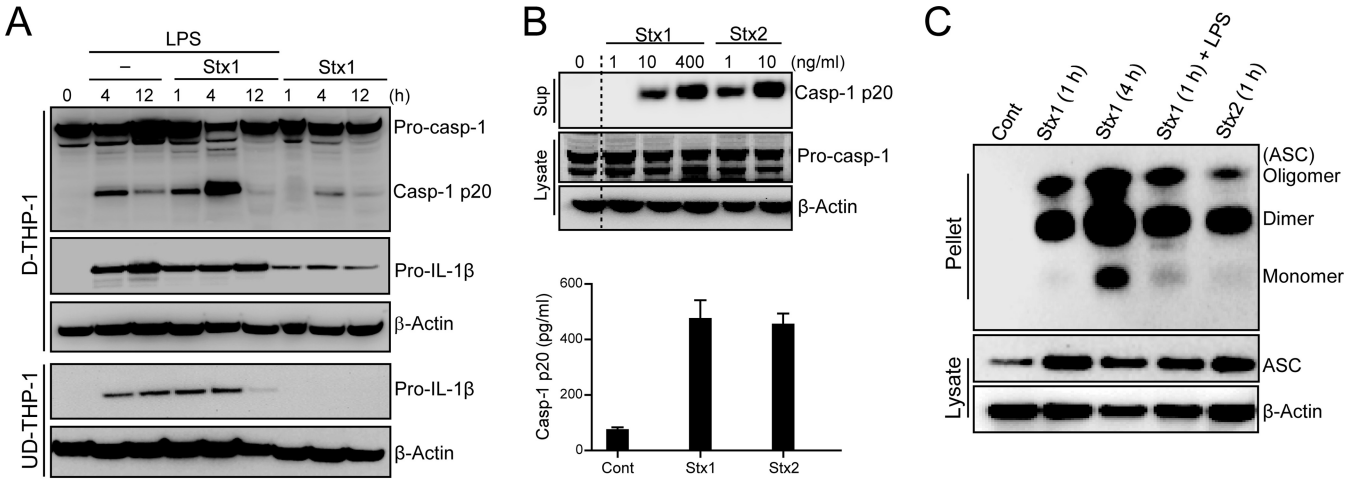

FIG 3 LPS augments Stx-mediated inflammasome activation and Stxs activate NLRP3-inflammasome via ASC oligomerization. (A) Effect of Stx1 on inflammasome activation in D-THP-1 cells. D-THP-1 cells or UD-THP-1 cells (2.0×10^6 cells per well) were treated with Stx1 (400 ng/ml) in the absence or presence of LPS (200 ng/ml). Cellular lysates were collected, followed by Western blotting with caspase-1- or IL-1β-specific antibodies. Membranes were stripped and reprobed with anti-β-actin antibody as a control for equal protein loading. The data shown are representative blots from two independent experiments. (B) Toxin-mediated caspase-1 activation. Cells were treated with Stx1 or Stx2 for 12 h. Supernatants then were analyzed for the presence of secreted Casp-1 p20 by Western blotting (upper) and ELISA (lower). Results are means ± SEM from two experiments, each performed in triplicate. (C) Stx-mediated ASC oligomerization. Western blot of oligomeric ASC pyroptosomes in DSS-cross-linked cell pellets of toxin-treated D-THP-1 cells in the presence or absence of LPS. Soluble cell lysates were immunoblotted with anti-ASC or anti-β-actin antibodies. Cont, untreated control; Casp-1 p20, active form p20 subunit of caspase-1; Pro-casp-1, procaspase-1; Pro-IL-1β, unprocessed pro-form of IL-1β.

Stx-mediated inflammasome activation is dependent on the toxin receptor Gb3. Binding of Stxs to the membrane receptor Gb3 is a prerequisite for initial cellular signaling events, leading to internalization, retrograde intracellular transport, and ultimately activation of multiple stress responses and proinflammatory cytokine production (48). Accordingly, we examined the effect of Gb3 on Stx-induced caspase-1 activation. Pretreatment of D-THP-1 cells with the glycosphingolipid synthesis inhibitor PDMP, which efficiently reduces Stx endocytic uptake and intracellular transport from endosomes to the Golgi apparatus (49), significantly reduced Gb3 expression (Fig. 4A, left) and attenuated Stx-mediated caspase-1 activation in a dose-dependent manner (Fig. 4A, right). Notably, toxin-mediated IL-1β secretion was undetectable in the crypt-like colon carcinoma-derived T84 cell line, which does not express Gb3 (Fig. 2). To obtain further evidence that Stx-induced inflammatory activation is dependent on Gb3, we measured the secretion of immunoreactive IL-1β from toxin-treated cells in the presence of PDMP. PDMP significantly decreased IL-1β secretion from toxin-treated cells (Fig. 4B). These results demonstrate that Gb3-mediated toxin binding and endocytosis are necessary for inflammasome activation, leading to the activation of caspase-1 and release of IL-1β production, in D-THP-1 cells.

Enzymatically functional Stxs are required for NLRP3 inflammasome activation. Retrograde transport of Stxs to the ER lumen, processing of the toxin to generate the enzymatically active A1 fragment, and translocation of this fragment across the ER membrane all are required for the depurination reaction of 28S rRNA and subsequent activation of ribotoxic stress responses (16). Therefore, we asked whether the delivery of enzymatically active Stxs into the cytosol is essential for the activation of the NLRP3 inflammasome. To determine the involvement of Stx enzymatic activity in the activation of caspase-1, we treated D-THP-1 cells with active Stx1, active Stx2, variants lacking enzy-

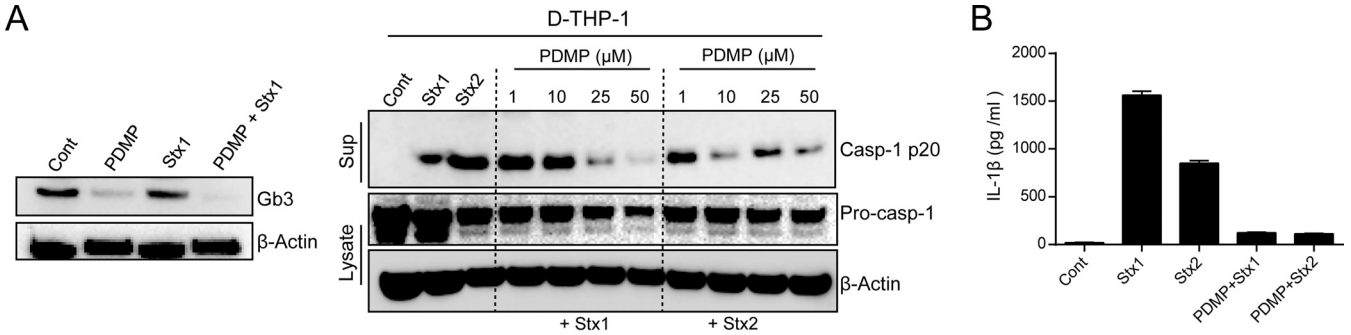

FIG 4 Stx-mediated inflammasome activation is dependent on the receptor Gb3. (A) Stx receptor Gb3 (left) and Casp-1 p20 (right) levels in toxin-treated D-THP-1 cells after pretreatment with the glucosylceramide synthetase inhibitor D-*threo*-PDMP. (B) Mature IL-1β levels in supernatants collected from toxin-treated D-THP-1 cells, with or without PDMP pretreatment, measured by sandwich ELISA. Standards provided with ELISA kits were used to calculate amounts of soluble cytokine protein. Cells were treated with 50 μM D-*threo*-PDMP, 400 ng/ml Stx1, or 10 ng/ml Stx2 unless otherwise indicated.

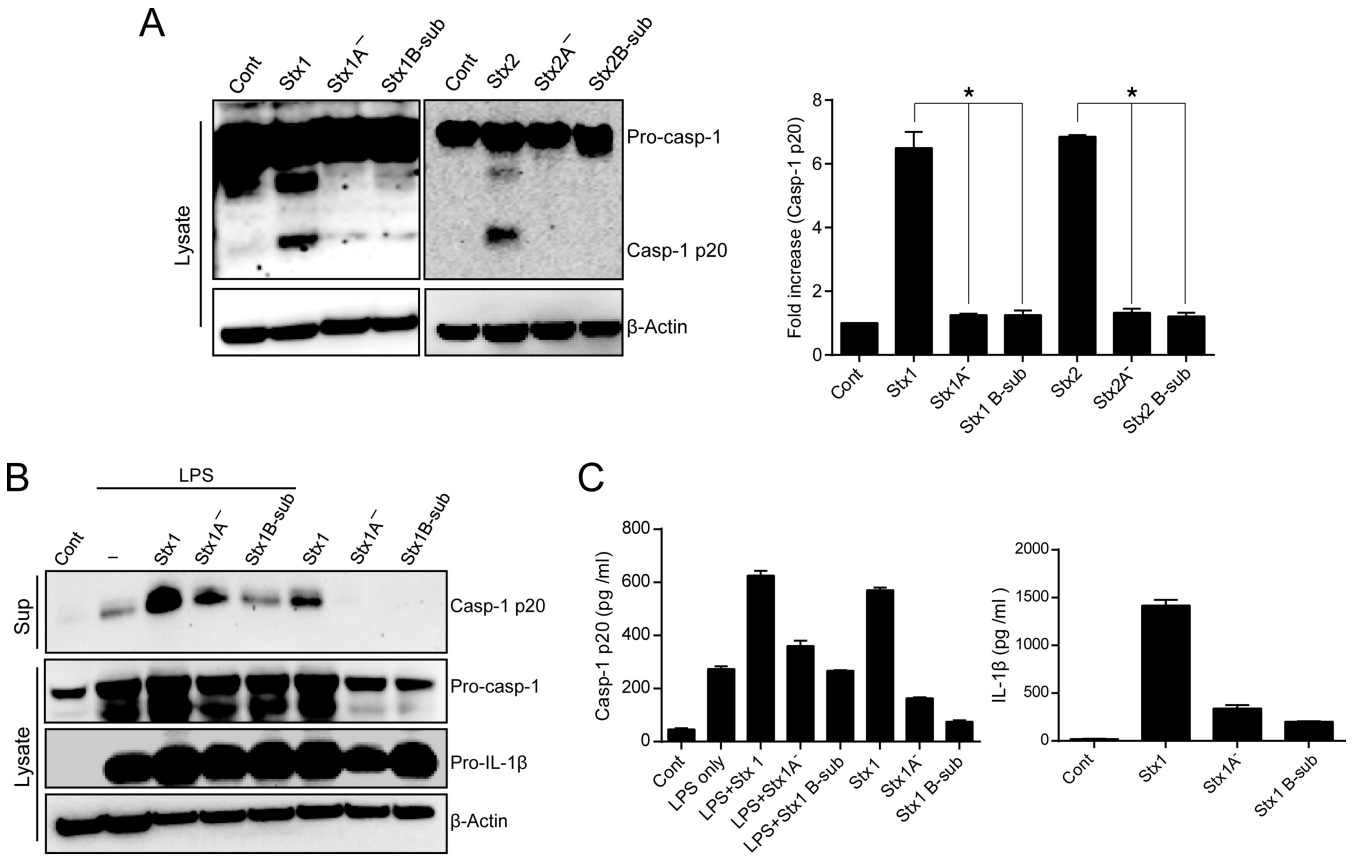

FIG 5 *N*-glycosidase activity of Stxs is required for NLRP3 inflammasome activation. (A) Caspase-1 was activated only by enzymatically functional toxins. D-THP-1 cells were treated with Stx1 (400 ng/ml), Stx1A$^-$ (400 ng/ml), Stx1 B subunits (400 ng/ml), Stx2 (10 ng/ml), Stx2A$^-$ (10 ng/ml), or Stx2 B subunits (10 ng/ml) for 4 h. (Left) Cell lysates were assessed for levels of procaspase-1 (Pro-casp-1) and the active form of caspase-1 (Casp-1 p20) following solubilization, fractionation by SDS-PAGE, and analysis by Western blotting. (Right) Bar graph depicts quantitation (means ± SEM) of the Casp-1 p20 level from three independent experiments. An asterisk indicates significant differences in Casp-1 p20 levels ($P < 0.001$). (B) Active caspase-1 (Casp-1 p20) released from enzymatically active Stx1-treated cells without LPS priming. D-THP-1 cells were pretreated with LPS or not pretreated and then were treated with Stx1, Stx1A$^-$, or Stx1 B subunits for 12 h. Western blotting of caspase-1 was used to reveal the release of processed Casp-1 p20 subunit into the supernatant. Cell lysates from LPS-primed or nonprimed cells were assessed for the production of procaspase-1 (Pro-casp-1) or Pro-IL-1β. Actin was used as the loading control. Western blots are representative of results from three separate experiments. (C) Levels of secreted active Casp-1 p20 and IL-1β from the toxin-treated D-THP-1 cells. Cells were stimulated with Stx1 (400 ng/ml), Stx1A$^-$ (400 ng/ml), or Stx1 B subunits (400 ng/ml) for 24 h in the presence or absence of LPS (200 ng/ml). Culture supernatants (media) were analyzed for secreted soluble Casp-1 p20 (left) and IL-1β (right) by ELISA. Values are expressed as means ± SEM from three independent experiments.

matic activity due to mutations in the A subunit catalytic residue of each toxin (StxA1$^-$ and StxA2$^-$), pentameric StxB1 subunit (Stx1B-sub), or StxB2 subunit (Stx2B-sub). The results revealed that only enzymatically active toxins promoted caspase-1 activation, whereas no activation was observed in cells treated with enzymatically deficient mutant toxins or the B subunits (Fig. 5A). LPS induced the release of active caspase-1 regardless of Stx treatment, and in combination with enzymatically active Stx1, LPS exerted a substantial synergistic effect on caspase-1 secretion (Fig. 5B). A significant amount of released caspase-1 was observed only in Stx1-treated cells. Notably, treatment with Stx1, Stx1A$^-$, and StxB1 subunits, with or without LPS, did not impair the production of inactive procaspase-1 and pro-IL-1β (Fig. 5B). Because active caspase-1 typically is secreted along with cytokines, we measured the levels of released caspase-1 and IL-1β by ELISA. Compared to wild-type Stx1 treatment, stimulation of D-THP-1 cells with StxA1$^-$ or StxB1 subunits significantly decreased the release of active caspase-1 and mature IL-1β into the media (Fig. 5C). We observed no significant synergistic effects of LPS priming on the release of active caspase-1 relative to treatment with wild-type Stx1 alone (Fig. 5C, left). Collectively, these data indicate that enzymatically functional Stxs are required for NLRP3 inflammasome to release proinflammatory cytokine IL-1β from D-THP-1 cells in an LPS-independent manner.

Stx-mediated upregulation of NLRP3 and ASC expression is required for inflammasome activation. An intrinsic inflammasome-activating state in macrophages is characterized by an elevated basal level of NLRP3 and ASC (50, 51). Therefore, we evaluated the expression of NLRP3 and ASC in Stx-sensitive D-THP-1 cells. Based on our finding that Stxs dominantly activate NLRP3 inflammasome to induce IL-1β production, we utilized quantitative real-time PCR and Western blotting to measure changes in mRNA and protein levels of NLRP3 and ASC after treatment of D-THP-1 cells with Stx1 or Stx2 for 0 to 4 h. Significant upregulation of ASC and NLRP3 was observed at transcriptional (Fig. 6A) and translational levels (Fig. 6B and C), relative to

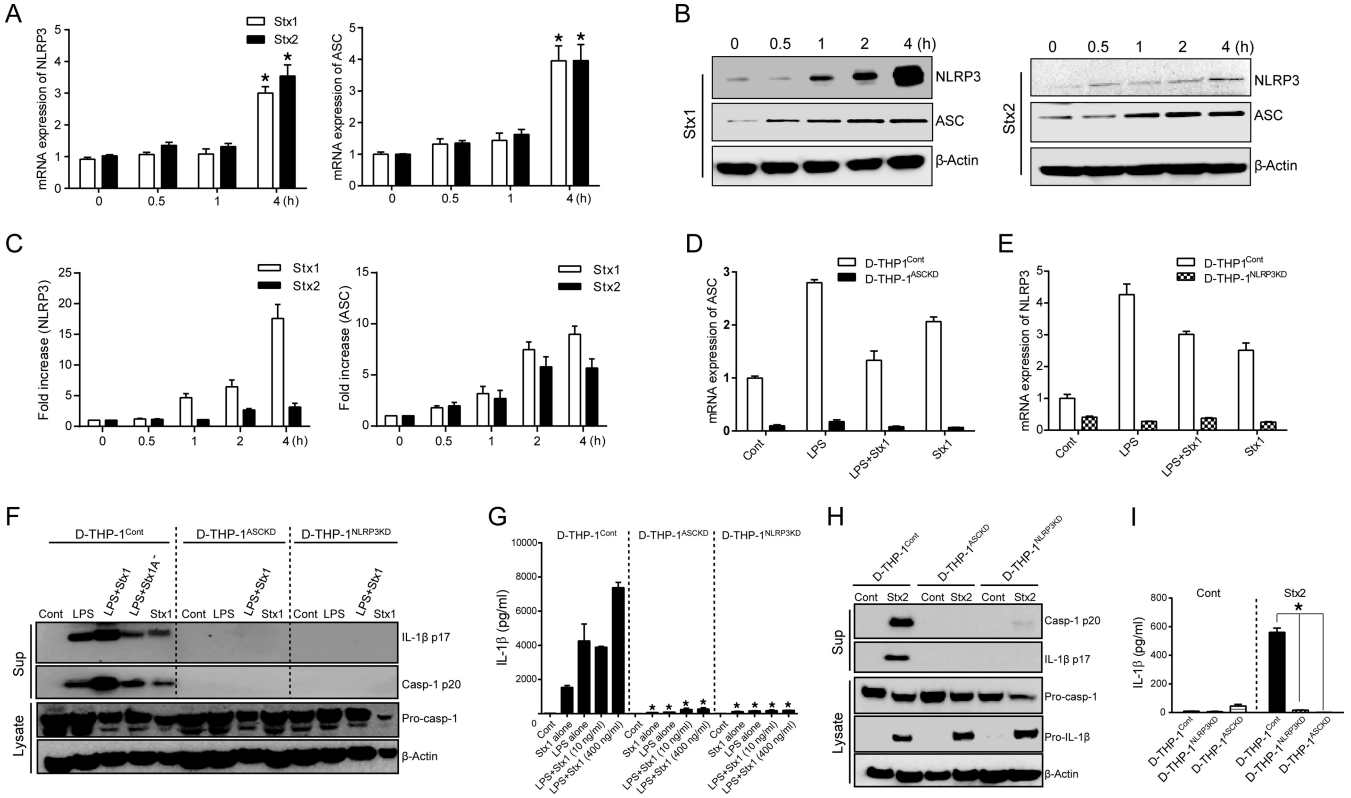

FIG 6 Stxs upregulate the expression of NLRP3 and ASC to activate the inflammasome. (A) NLRP3 and ASC mRNA levels in THP-1 cells following intoxication with Stx1 or Stx2. Cells were stimulated with Stx1 (400 ng/ml) or Stx2 (10 ng/ml) for the indicated times. Total RNA was isolated and treated with DNase, and cDNA was synthesized. Quantitative real-time PCR was performed with primers specific for human NLRP3, ASC, and β-actin. Relative mRNA expression was calculated by using the delta threshold cycle (ΔC_T) method. Data represent mean fold induction ± SEM from three independent experiments. Statistical significance was calculated by two-way ANOVA (*, $P < 0.01$ compared to results at 0 h). (B) Protein levels of NLRP3 and ASC expressed in D-THP-1 cells intoxicated with Stx1 or Stx2. Cells were treated with Stx1 or Stx2 for the indicated times. Whole-cell lysates (50 μg) were subjected to SDS-PAGE on 4 to 15% gels, blotted, and probed with specific antibodies against human NLRP3, ASC, and actin (used as a loading control). The blot shown is representative of three independent experiments. (C) Quantitative analysis (means ± SEM) of NLRP3 (left) or ASC (right) production from three independent experiments. (D and E) mRNA levels of ASC (left) and NLRP3 (right) expressed in wild-type D-THP-1 (D-THP-1^{Cont}), D-THP-1 cells with stable knockdown of ASC expression (D-THP-1^{ASCKD}), and D-THP-1 cells with stable knockdown of NLRP3 mRNA expression (D-THP-1^{NLRP3KD}) after exposure to Stx1 and/or LPS. (F) Stx1- or Stx2-mediated caspase-1 activation and IL-1β secretion require NLRP3 inflammasome function. Pro-caspase-1 (Pro-casp-1), activated caspase-1 (Casp-1 p20), mature soluble IL-1β (IL-1β p17), and β-actin (loading control) levels were measured by Western blotting of lysates or cell-free supernatants (media) prepared from wild-type D-THP-1 cells (D-THP-1^{Cont}), D-THP-1 cells with stable knockdown of ASC expression (D-THP-1^{ASCKD}), or D-THP-1 cells with stable knockdown of NLRP3 expression (D-THP-1^{NLRP3KD}) after exposure to Stx1 or Stx1A$^-$ in the presence or absence of LPS. (G) Measurement of mature IL-1β (IL-1β p17) levels by ELISA in cell-free supernatants from D-THP-1^{Cont}, D-THP-1^{ASCKD}, and D-THP-1^{NLRP3KD} cells stimulated with Stx1 (10 or 400 ng/ml) for 24 h in the presence or absence of LPS. Standards provided with the ELISA kits were used to calculate amounts of cytokine protein. Values are expressed as means ± SEM from two independent experiments performed in triplicate. Asterisks indicate a statistically significant difference relative to D-THP-1^{Cont} values ($P < 0.01$). (H) Analysis of active Casp-1 p20 and IL-1β p17 secreted from cells treated with Stx2 (10 ng/ml). (I) Measurement of IL-1β released from cells exposed to Stx2 (10 ng/ml) for 24 h, as determined by ELISA. Results are means ± SEM from two independent experiments performed in triplicate. Asterisks indicate a statistically significant difference relative to results for D-THP-1 ($P < 0.01$).

results for untreated control cells, after 4 h treatment with the toxins. Purified Stx1 or Stx2 reproducibly increased total levels of NLRP3 or ASC protein relative to those at 0 h (Fig. 6C, bar graph). These results suggest that Stxs induce the upregulation of NLRP3 and ASC, which are necessary to facilitate inflammasome assembly and activation.

Using D-THP-1 cells in which NLRP3 or ASC were stably knocked down, we expanded our understanding of NLRP3 inflammasome-mediated production of IL-1β in response to Stxs. Consistent with the deficiency of NLRP3 or ASC in these knockdown cells, we observed no induction of NLRP3 or ASC at the transcriptional level following LPS or Stx1 treatment (Fig. 6D and E). To ensure that the Casp-1 p20 and IL-1β release observed upon Stx1 intoxication resulted from NLRP3 inflammasome activation, we exposed D-THP-1 cells with stable deficiencies in NLRP3 (D-THP-1^{NLRP3KD}) or ASC (D-THP-1^{ASCKD}) to the toxin and compared their responses to those of wild-type D-THP-1 cells (D-THP-1^{Cont}). The active caspase-1 and IL-1β secretion in supernatants from D-THP-1 cells were detected following Stx1 treatment, as well as after LPS-primed-Stx1 and StxA1$^-$ treatment. However, all treatments failed to trigger caspase-1 autoprocessing and IL-1β secretion in cells lacking ASC or NLRP3 (Fig. 6F). Concentrations of IL-1β secreted into culture supernatants from D-THP-1^{Cont} cells treated with Stx1 alone, as well as LPS-primed Stx1-treated cells, were significantly elevated, whereas greatly reduced secretion of IL-1β was observed from the D-THP-1^{ASCKD} and D-THP-1^{NLRP3KD} cells that received the same treatments as wild-type cells (Fig. 6G). Comparable results were obtained from Stx2-treated cells (Fig. 6H

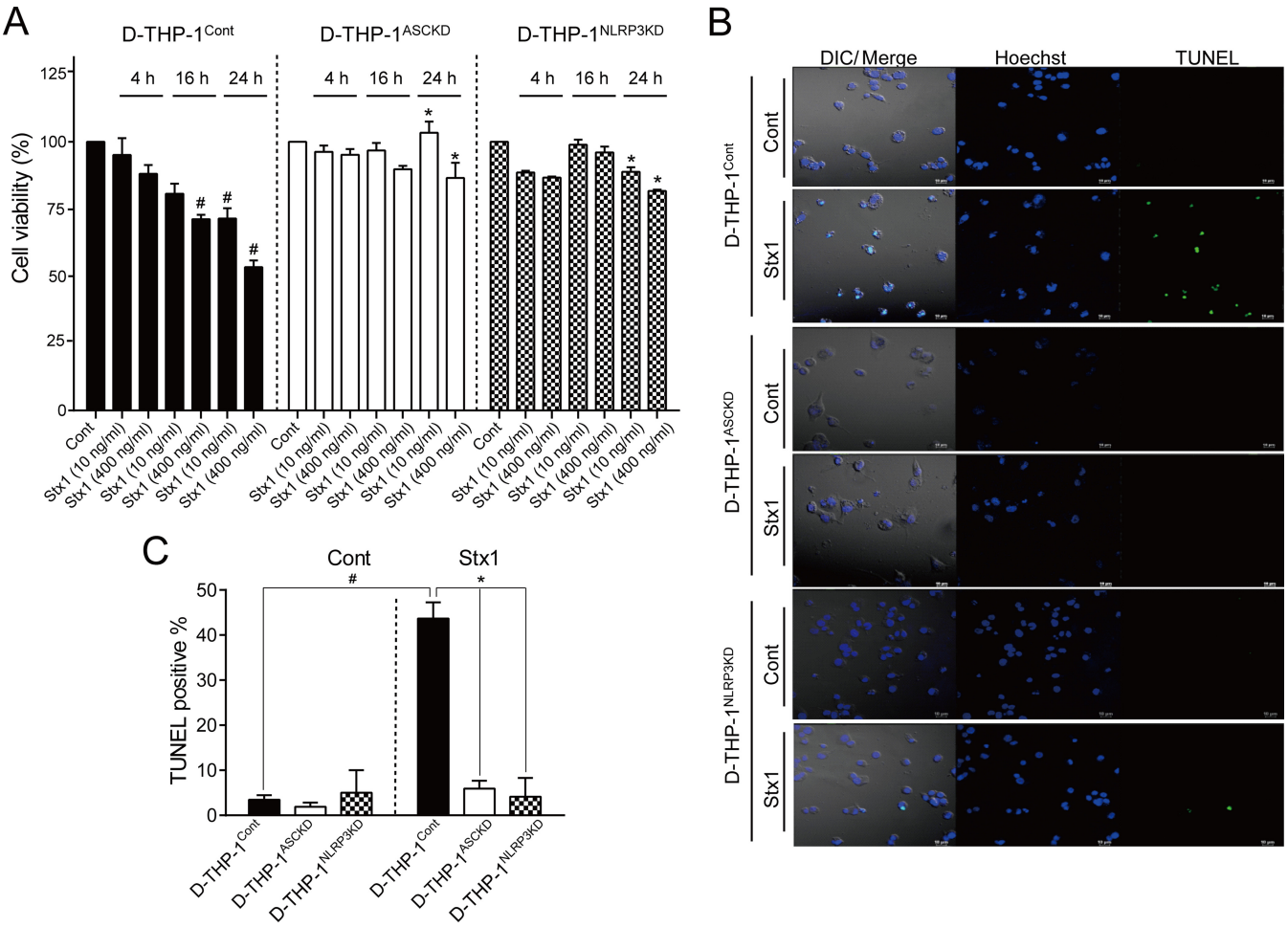

FIG 7 NLRP3 inflammasome deficiency increases toxin resistance. (A) Effect of Stx1 on cell viability. Wild-type D-THP-1 (D-THP-1^{Cont}), D-THP-1^{ASCKD}, and D-THP-1^{NLRP3KD} cells were seeded in 96-well microtiter plates and incubated alone (Cont) or with Stx1 (10 or 400 ng/ml) for 24 h. Cell viability was measured by colorimetric assay using MTS dye. Data are expressed as percent viability relative to that of untreated control cells at each time point. Results shown are means ± SEM from two independent experiments using triplicate samples. (B) Effect of Stx1 on apoptosis. D-THP-1^{Cont}, D-THP-1^{ASCKD}, and D-THP-1^{NLRP3KD} cells were treated with Stx1 (400 ng/ml) for 24 h. Cells were fixed, permeabilized, and incubated with TUNEL reaction solution. Representative TUNEL-positive cells visualized by fluorescence microscopy are shown. Ten different fields (magnification, ×20) for each treatment were selected to count total numbers of TUNEL-positive cells. Total numbers of cells per field (magnification, ×20) also were counted, and the percentage of apoptotic cells (above the value for untreated controls) was calculated as described in Materials and Methods. (C) Quantitative data showing the percentage of apoptosis (means ± SEM from at least two independent experiments for each treatment condition). #, significant difference ($P < 0.001$) for D-THP-1 cells treated with Stx1 versus untreated cells; *, significant difference ($P < 0.001$) for control cells treated with Stx1 versus ASC- or NLRP3-deficient cells treated with Stx1. Cont, untreated cells.

and I). Collectively, these data further suggest that caspase-1 autoprocessing and IL-1β secretion following Stx intoxication rely critically on NLRP3 and ASC for inflammasome activation.

Stx-mediated NLRP3 inflammasome signaling induces both pyroptosis and apoptosis in parallel. NLRP3 and AIM2 inflammasomes may induce pyroptosis and apoptosis in association with the processing of caspase-8/3 (52). It is also important to note that many cell types appear to be particularly sensitive to the induction of apoptosis via ribotoxic stress responses activated by Stxs in the context of sublethal protein synthesis inhibition (17). To determine whether Stx1 can promote NLRP3 inflammasome-dependent cell death, we exposed wild-type D-THP-1^{Cont}, D-THP-1^{ASCKD}, and D-THP-1^{NLRP3KD} cells to the toxin for 0 to 24 h and assessed cell viability. D-THP-1^{Cont} cells treated with Stx1 (400 ng ml^{-1}) for 24 h were 53% viable, whereas toxin-treated D-THP-1^{ASCKD} and D-THP-1^{NLRP3KD} cells were 94% and 80% viable, respectively, at 24 h (Fig. 7A), implying that a deficiency in NLRP3 inflammasome-driven IL-1β production protects cells from Stx1 cytotoxicity. To further evaluate NLRP3 inflammasome-dependent cell death triggered by Stx1, we explored apoptosis induction by subjecting cells to TUNEL staining after 24 h of toxin exposure. TUNEL fluorescence intensity in toxin-treated cells was decreased by the depletion of NLRP3 and ASC (Fig. 7B). Statistical analysis of TUNEL-positive cells in Stx1-treated D-THP-1^{ASCKD} and D-THP-1^{NLRP3KD} cells revealed that the frequency of apoptotic cell death was significantly reduced relative to that in toxin-treated D-THP-1^{Cont} cells (Fig. 7C). These data suggest that NLRP3 inflammasome signaling is involved in the apoptotic death pathway in Stx1-treated macrophage-like cells. Accordingly, we reasoned that if D-THP-1^{ASCKD} or D-THP-1^{NLRP3KD} cells are protected against Stx1, caspase-8/3 activation should be decreased by NLRP3 or ASC depletion. To evaluate the role of caspase activa-

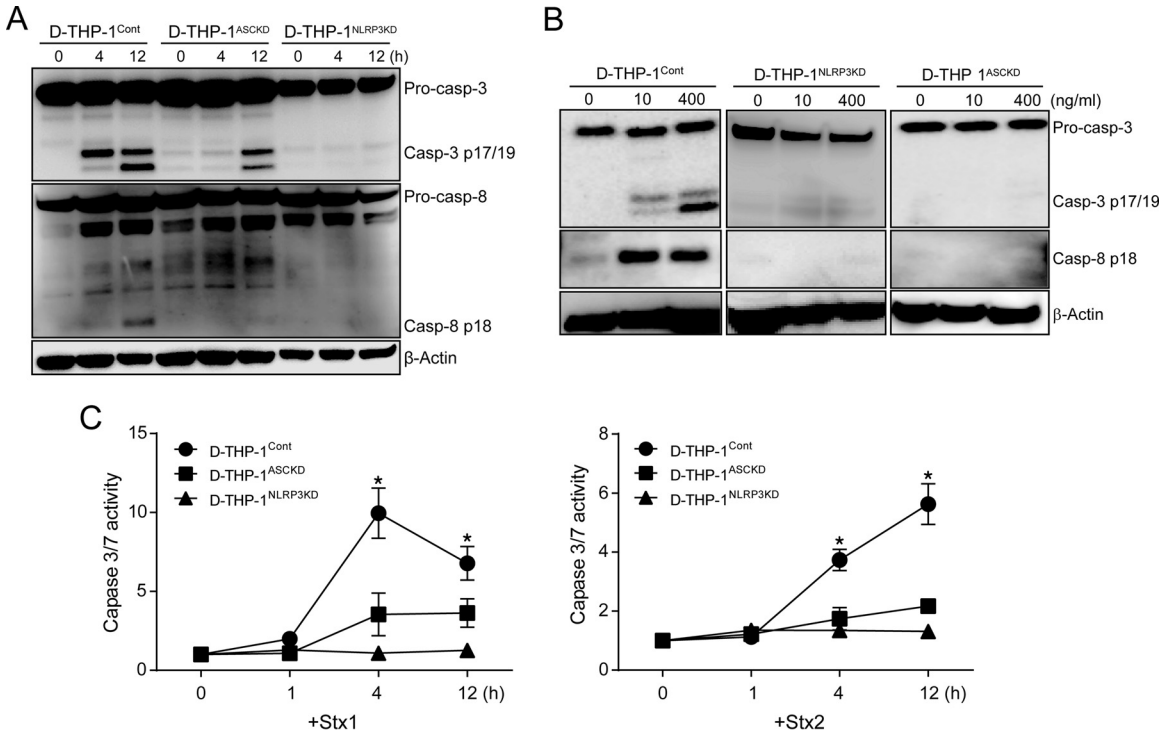

FIG 8 Stxs activate apoptotic caspases in an ASC- and NLRP3-dependent manner. (A) D-THP-1^{Cont}, D-THP-1^{ASCKD}, and D-THP-1^{NLRP3KD} cells were treated with Stx2 (10 ng/ml) for 0 to 12 h. Cells were collected, washed with PBS, and lysed. Total protein concentrations were determined, and equal amounts of total protein (50 μg) were separated by SDS-PAGE on 12% Tris-glycine gels. Cleavages of caspase-3 and caspase-8 were detected using caspase-specific antibodies. β-Actin was used as a control for equal protein loading. The immunoblots are representative of three independent experiments. (B) Effect of Stx1 on caspase activation in D-THP-1^{Cont}, D-THP-1^{ASCKD}, and D-THP-1^{NLRP3KD} cells. Cells were treated with Stx1 for 4 h. Cells were collected, washed with PBS, and lysed with CHAPS modified lysis buffer supplemented with protease and phosphatase inhibitors. Total protein concentrations were determined, and equal amounts of total protein (50 μg) were separated by 12% Tris-glycine SDS-PAGE. Cleavages of caspase-3 and caspase-8 were detected by Western blotting using caspase-specific antibodies. β-Actin was used as a control for equal protein loading. Immunoblots are representative of three independent experiments. Pro-casp-3, procaspase-3; Casp-3 p17/19, active form of caspase-3; Pro-casp-8, procaspase-8; Casp-8 p18, active form of caspase-8. (C) Measurement of caspase-3/7 activity in D-THP-1^{Cont}, D-THP-1^{ASCKD}, and D-THP-1^{NLRP3KD} cells in the presence of Stx1 (400 ng/ml; left) or Stx2 (10 ng/ml; right) relative to the control group (0 h). Data presented are means ± SEM from at least three independent experiments. $P < 0.001$ (*) was considered to indicate statistical significance in comparisons of Stx1 or Stx2-treated D-THP-1 ^{Cont} cells to the D-THP-1^{ASCKD} and D-THP-1^{NLRP3KD} cells at each time point.

tion in NLRP3 inflammasome-dependent apoptosis, wild-type D-THP-1^{Cont}, D-THP-1^{ASCKD}, and D-THP-1^{NLRP3KD} cells were treated with Stx2 for 0 to 12 h. The knockdown of ASC or NLRP3 significantly reduced caspase-8/3 cleavage in response to Stx2 (Fig. 8A). We also observed that deficiency in the NLRP3 inflammasome almost completely abrogated Stx1-induced caspase-3/7 activation (Fig. 8B). By using specific colorimetric substrates, we consistently observed significantly increased caspase-3/7 activities in Stx1- or Stx2-treated wild-type D-THP-1^{Cont} cells (Fig. 8C). In contrast, D-THP-1^{ASCKD} and D-THP-1^{NLRP3KD} cells did not exhibit significant caspase-3/7 activities in response to the toxins (Fig. 8C). These results suggest that NLRP3 inflammasome signaling in Stx-intoxicated cells activates caspase-8/3 processing and initiates apoptosis, in addition to initiating the caspase-1-dependent pyroptotic cell death pathway.

DISCUSSION

Dysregulation of cytokine expression contributes to the development of chronic inflammatory diseases such as rheumatoid arthritis (53) and serious acute complications of infection such as septic shock (54). Stxs are major virulence factors that contribute to the ability of STEC to intoxicate and injure host cells, and Stx-mediated proinflammatory responses may potentiate cell or tissue damage in a localized manner, such as in in the case of glomerular microvascular endothelial cells (55). One of the key challenges in understanding the pathogenesis of Stx-mediated disease is deciphering the mechanisms underlying the dysregulation of pro- and anti-inflammatory responses in toxin-resistant and toxin-sensitive host cells. Stxs regulate cytokine expression at the transcriptional stage through the transcription factors NF-κB, AP-1, and Egr-1 (25, 26, 41), as well at the posttranscriptional stage through phosphorylation of eukaryotic translational initiation factors (56). Stxs trigger a ribotoxic stress response leading to the activation of three major MAPK signaling pathways (JNK, p38, and ERK), which in turn regulate cytokine and chemokine expression in macrophage-like THP-1 cells (42, 56). Furthermore, Stx1 alters the phosphorylation status of MAPKs, leading to differential MAPK activation and cytokine and chemokine expression by induction of the dual-specificity phosphatase DUSP1 in D-THP-1 cells (42).

Here, we show that Stxs induce the processing of pro-IL-1β to mature IL-1β in an NLRP3 inflammasome-dependent manner in human macrophage-like cells, further supporting recent studies showing that the suppression of ribosomal function by a variety of protein synthesis inhibitors (including ricin, cycloheximide, pu-

romycin, pactamycin, and anisomycin) leads to IL-1β-dependent inflammation via activation of the NLRP3 inflammasome (31, 38). To intoxicate and thereby promote a proinflammatory response in multiple Gb3-expressing cell types, Stxs must bind the toxin receptor, become internalized, and then be routed via early/recycling endosomes to the *trans*-Golgi network to reach the ER lumen (48, 57–59). In epithelial cells, Stxs produced by *E. coli* induce apoptosis only in Gb3-expressing cells via a mechanism involving regulation by members of the Bcl-2 protein family (60). Apoptosis through this mechanism was not induced in Gb3-deficient T84 cells (60), although in this cell type, the existence of an alternative receptor for Stxs or nucleolar trafficking of the toxin via a carrier-dependent process has been proposed (61). Following similar logic, we hypothesized that the inhibition of Gb3 synthesis in Gb3-expressing D-THP-1 cells would result in decreased NLRP3 inflammasome activation following intoxication by Stxs. Procaspase-1 activation and subsequent processing of IL-1β were markedly suppressed in the presence of the Gb3 inhibitor PDMP (Fig. 4). Harrison et al. suggested that the presence of the intact A subunit of Stx1 is necessary for the induction of IL-1β protein in D-THP-1 cells (62). Consistent with this, toxin preparations lacking enzymatic activity (Stx A subunit toxoids or purified B subunits) failed to trigger procaspase-1 activation or soluble IL-1β production (Fig. 5). Taken together, these studies suggest that toxin binding to Gb3, retrograde transport, retrotranslocation of the processed Stx A1-fragments across the ER membrane, and enzymatic action on the 28 rRNA all are required for NLRP3 inflammasome-mediated induction of caspase-1 activation and subsequent IL-1β secretion. Furthermore, we showed that treatment of D-THP-1 cells with LPS or Stx1 alone activated procaspase-1 (Fig. 5). However, optimal activation of procaspase-1 occurred in cells treated with both LPS and Stx1 (Fig. 5B and C), suggesting that the presence of LPS in the bloodstream, which may occur after structural or functional damage to the colon associated with *S. dysenteriae* serotype 1 or STEC infections, augments proinflammatory cytokine production, leading to increased localized vascular damage.

Among numerous inflammasome activators, the NLRP3 inflammasome is strongly activated by a large number of bacterial toxins (63–66). One important conceptual question that remains to be addressed is whether receptor-mediated internalization of Stxs or the retrotranslocation of functional StxA1 fragments across the ER membrane could be recognized by cytosolic receptors such as NLR inflammasome sensors. In this study, we show that transient silencing of NLRP3 and ASC expression by siRNAs dramatically reduced Stx1-mediated inflammasome activation, as reflected by procaspase-1 processing and soluble IL-1β production (Fig. 1). In contrast, Stx1 treatment of cells following silencing of NLRC4 or AIM2 expression resulted in levels of caspase and IL-1β processing comparable to those in cells treated with nontargeting siRNA (Fig. 1). We verified these results in THP-1 cells with stable deficiencies in NLRP3 and ASC expression (Fig. 6F to I). Together, these data suggest that Stx-mediated inflammasome activation leading to IL-1β production is restricted to NLRP3 inflammasomes in macrophage-like THP-1 cells, although experiments examining the role of inflammasomes in activating the production of a wider panel of cytokines/chemokines are clearly warranted.

Bauernfeind et al. demonstrated that NF-κB activation is necessary for the expression of NLRP3, and the NLRP3 inflammasome is activated in an NLRP3 level-dependent manner in conjunction with a second stimulus, such as ATP or crystals (67). Importantly in this regard, Stxs capable of inhibiting protein synthesis activate the transcription factors AP-1, NF-κB, and Egr-1 (25, 26, 68). Using a combination of immunoblotting and quantitative RT-PCR analyses, we demonstrated that the amounts of ASC and NLRP3 at both the mRNA and protein levels were elevated in macrophage-like THP-1 cells following Stx1 or Stx2 treatment (Fig. 6A to C). These data suggest that transcription of the genes encoding the inflammasome components NLRP3 and ASC is not impaired during intoxication, and indeed, within 4 h of toxin treatment, their transcript levels were significantly elevated; however, transcription and translation did not appear to be directly correlated. Although both Stx1 and Stx2 appeared capable of inducing NLRP3 and ASC transcripts, Stx1 was a better inducer of NLRP3 and ASC production than Stx2. Differences between the effects of these toxins on NLRP3 and ASC production correlated with differences in the soluble IL-1β level induced by Stx1 and Stx2 (compare Fig. 6G to I). Epidemiological studies have suggested that infections with STEC expressing Stx2 are associated with the development of the majority of life-threatening extraintestinal complications, such as HUS (4, 69), and a comparative study of toxicities using mice revealed that purified Stx2 is a more potent toxin than Stx1 (5). However, in the baboon, an animal model that most closely reproduces the disease seen in humans, Stx1 challenge revealed a stronger proinflammatory response, while the proinflammatory response elicited by Stx2 was gradual and delayed (70). The reason for the differences in proinflammatory responses between Stx1 and Stx2 in animal models remains to be clarified.

The role of the inflammasome in activating apoptotic cell death has been largely overlooked due to the rapid induction of pyroptosis by other stimuli. Recently, Pierini et al. showed that apoptotic responses triggered through AIM2 inflammasome activation may be involved in macrophage cell death induced by *Francisella tularensis* (71). Another study demonstrated that in murine macrophages, NLRC4- and ASC-dependent cleavage of procaspase-3 generates functional executioner caspase-3 in response to *Legionella pneumophila* infection (72). Furthermore, Sagulenko et al. suggested that the activation of AIM2 and NLRP3 inflammasomes induces both apoptotic and pyroptotic cell death pathways, leading to the activation of the executioner caspases, caspase-8 and caspase-3 (52). We showed here that Stx1 induces cell death in D-THP-1 cells. This cell death was mediated by apoptosis, as indicated by the elevated numbers of TUNEL-positive cells following toxin treatment (Fig. 7). The induction of the apoptotic response by Stx1 may be regulated by the NLR adaptor proteins ASC and NLRP3, as evidenced by the resistance of D-THP-1^{ASCKD} and D-THP-1^{NLRP3KD} cells to the cytotoxic action of Stx1 and the reduced cleavage of procaspase-3 and procaspase-8 in toxin-treated D-THP-1^{ASCKD} and D-THP-1^{NLRP3KD} cells (Fig. 8).

Taken together, the data presented here support a model of Stx-induced IL-1β production and cell death signaling through caspase activation, as outlined in Fig. 9. Our data support a model in which the Stx A1 fragments are retrotranslocated into the cytoplasm, perhaps leading to ribotoxic stress resulting in the assembly of functional NLRP3 inflammasome. This, in turn, activates executioner caspases involved in processing of IL-1β as well as induction of apoptosis. Based on the observations that the variants

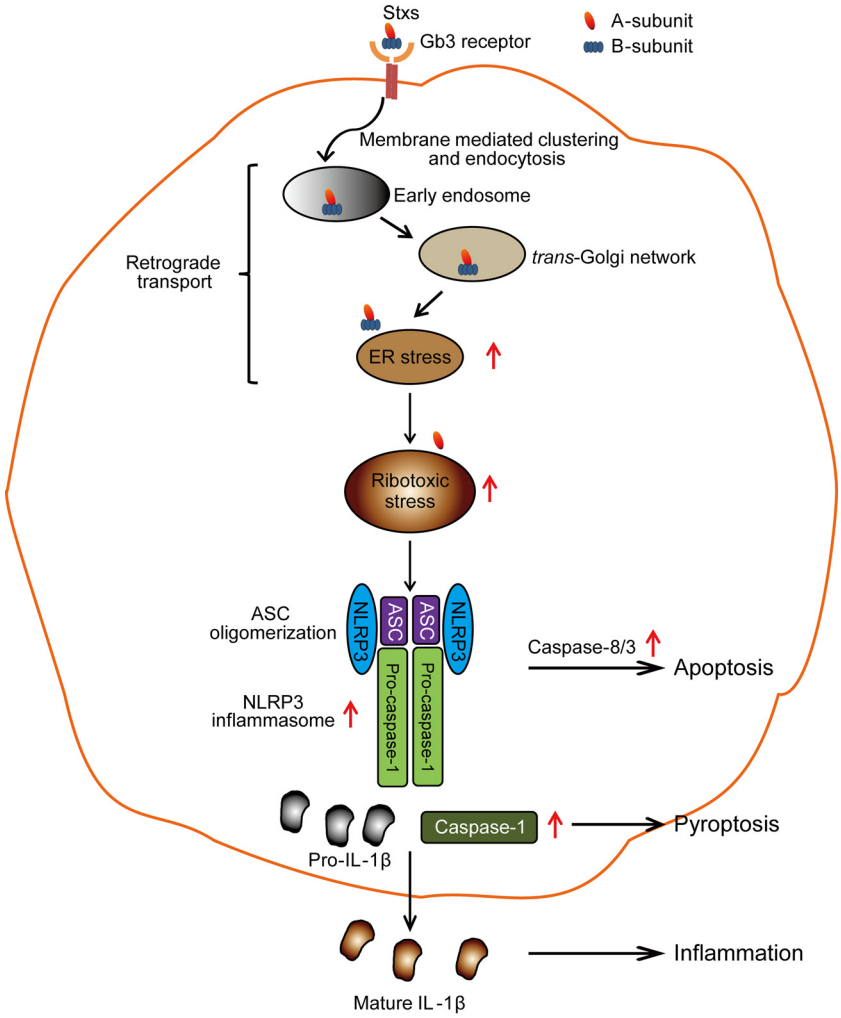

FIG 9 Model of Stx-mediated NLRP3 inflammasome activation leading to promotion of apoptotic and pyroptotic cell death. Stxs binding to Gb3 receptor on the surface of susceptible host cells undergo endocytosis, ER retrograde transport, processing of the A subunit to the enzymatically active A1 fragment, and translocation of this fragment into the cytosol, leading to ribotoxic stress. The resultant ribotoxic stress triggers the assembly of the NLRP3 inflammasome and activation of caspase-1, which is involved in the processing of IL-1β, as well as the apoptosis-inducing caspase-8 and caspase-3. These events promote apoptotic and pyroptotic cell death in parallel.

(StxA1$^-$ and StxA2$^-$) lacking enzymatic activity could not activate procaspase-1 and pro-IL-1β processing whereas their active counterparts could activate NLRP3 inflammasome-mediated procaspase-1 and pro-IL-1β processing (Fig. 5), Stx-induced ribotoxic stress responses may trigger NLRP3 inflammasome activation. In their original characterization of the mutant StxA1$^-$ with deficiency in *N*-glycosidase activity, Ohmura et al. showed that the mutant possessed approximately 1/300,000 of the cytotoxic activity of the active holotoxin in Vero cells (32). In addition, Smith et al. demonstrated that the Stx1 A subunit mutant lacking *N*-glycosidase activity was unable to activate p38MAPK and JNK in human intestinal epithelial cells through the ribotoxic stress mechanism, indicating that the enzymatic activity of the toxin is required to induce ribotoxic stress responses (73). A number of additional studies are necessary to fully characterize the cellular response to the toxins. For example, the upstream signaling events necessary for activation of the NLRP3 inflammasome machinery remain to be fully described. In addition, it remains unclear whether StxA1 fragment cytosolic unfolding and folding events, binding to the ribosome or ribosomal stalk, or enzymatic action at the ribosomal α-sarcin/ricin loop constitute the initial signal for inflammasome function. On the other hand, a recent study showed that Stx, a major virulence factor required for enterohemorrhagic *E. coli* (EHEC)-induced intestinal and renal disease, does not contribute to IL-1β production in murine bone marrow-derived macrophages (74). This study reported that EHEC-specific virulence factors, including Stx, are unessential for NLRP3 activation, while bacterial nucleic acids such as RNA-DNA hybrids and RNA mediate inflammasome-dependent responses (74), suggesting that the mouse BMDM used in this study is not sensitive to EHEC-specific virulence factors, including Stx.

Children and the elderly are at increased risk for developing life-threatening extraintestinal complications following the ingestion of Stx-producing bacteria. The current first-line medical therapy for treating bloody diarrhea, acute renal failure, and central nervous system complications caused by Stxs is entirely supportive, e.g., peritoneal dialysis or hemodialysis to support renal function in HUS. However, no vaccines exist to prevent these

diseases, and no available therapeutic regimens have been demonstrated to prevent or interrupt disease progression. An improved understanding of host cell signaling responses activated by Stxs will be necessary to identify novel targets for intervention in pathogenesis. Inhibition of Stx-mediated NLRP3-inflammasome signaling represents a novel strategy for preventing cell death and reducing proinflammatory cytokine production. The development and clinical testing of such approaches may ameliorate the major public health consequences of infections by *S. dysenteriae* serotype 1 and STEC.

ACKNOWLEDGMENTS

We thank Shinji Yamasaki for the gift of reagents necessary to carry out the experiments.

We have no financial conflicts of interest to report.

FUNDING INFORMATION

The KRIBB Initiative Program provided funding to Myung Hee Kim under grant number KGM4541521. National Research Foundation of Korea (NRF) provided funding to Myung Hee Kim under grant number 2014R1A2A1A01005971.

REFERENCES

1. **Proulx F, Tesh VL.** 2007. Renal diseases in the pediatric intensive care unit: thrombotic microangiopathy, hemolytic uremic syndrome, and thrombotic thrombocytopenia purpura, p 1189–1203. *In* Wheeler DS, Wong Hector R, Shanley TP (ed), Pediatric care medicine: basic science and clinical evidence. Springer-Verlag, London, United Kingdom.
2. **Weinstein DL, Jackson MP, Samuel JE, Holmes RK, O'Brien AD.** 1988. Cloning and sequencing of a Shiga-like toxin type II variant from Escherichia coli strain responsible for edema disease of swine. J Bacteriol **170:** 4223–4230.
3. **Strockbine NA, Marques LR, Newland JW, Smith HW, Holmes RK, O'Brien AD.** 1986. Two toxin-converting phages from Escherichia coli O157:H7 strain 933 encode antigenically distinct toxins with similar biologic activities. Infect Immun **53:**135–140.
4. **Tarr PI, Gordon CA, Chandler WL.** 2005. Shiga-toxin-producing Escherichia coli and haemolytic uraemic syndrome. Lancet **365:**1073–1086.
5. **Tesh VL, Burris JA, Owens JW, Gordon VM, Wadolkowski EA, O'Brien AD, Samuel JE.** 1993. Comparison of the relative toxicities of Shiga-like toxins type I and type II for mice. Infect Immun **61:**3392–3402.
6. **Fraser ME, Fujinaga M, Cherney MM, Melton-Celsa AR, Twiddy EM, O'Brien AD, James MN.** 2004. Structure of Shiga toxin type 2 (Stx2) from Escherichia coli O157:H7. J Biol Chem **279:**27511–27517. http://dx.doi.org/10.1074/jbc.M401939200.
7. **Fraser ME, Chernaia MM, Kozlov YV, James MN.** 1994. Crystal structure of the holotoxin from Shigella dysenteriae at 2.5 A resolution. Nat Struct Biol **1:**59–64. http://dx.doi.org/10.1038/nsb0194-59.
8. **Endo Y, Tsurugi K, Yutsudo T, Takeda Y, Ogasawara T, Igarashi K.** 1988. Site of action of a Vero toxin (VT2) from Escherichia coli O157:H7 and of Shiga toxin on eukaryotic ribosomes. RNA N-glycosidase activity of the toxins. Eur J Biochem **171:**45–50.
9. **Sandvig K, Garred O, Prydz K, Kozlov JV, Hansen SH, van Deurs B.** 1992. Retrograde transport of endocytosed Shiga toxin to the endoplasmic reticulum. Nature **358:**510–512. http://dx.doi.org/10.1038/358510a0.
10. **Garred O, Dubinina E, Holm PK, Olsnes S, van Deurs B, Kozlov JV, Sandvig K.** 1995. Role of processing and intracellular transport for optimal toxicity of Shiga toxin and toxin mutants. Exp Cell Res **218:**39–49. http://dx.doi.org/10.1006/excr.1995.1128.
11. **Garred O, van Deurs B, Sandvig K.** 1995. Furin-induced cleavage and activation of Shiga toxin. J Biol Chem **270:**10817–10821. http://dx.doi.org/10.1074/jbc.270.18.10817.
12. **Johannes L, Romer W.** 2010. Shiga toxins–from cell biology to biomedical applications. Nat Rev Microbiol **8:**105–116.
13. **Garred O, Dubinina E, Polesskaya A, Olsnes S, Kozlov J, Sandvig K.** 1997. Role of the disulfide bond in Shiga toxin A-chain for toxin entry into cells. J Biol Chem **272:**11414–11419. http://dx.doi.org/10.1074/jbc.272.17.11414.
14. **Tam PJ, Lingwood CA.** 2007. Membrane cytosolic translocation of verotoxin A1 subunit in target cells. Microbiology **153:**2700–2710. http://dx.doi.org/10.1099/mic.0.2007/006858-0.
15. **Sandvig K, van Deurs B.** 2002. Transport of protein toxins into cells: pathways used by ricin, cholera toxin and Shiga toxin. FEBS Lett **529:**49–53. http://dx.doi.org/10.1016/S0014-5793(02)03182-4.
16. **Iordanov MS, Pribnow D, Magun JL, Dinh TH, Pearson JA, Chen SL, Magun BE.** 1997. Ribotoxic stress response: activation of the stress-activated protein kinase JNK1 by inhibitors of the peptidyl transferase reaction and by sequence-specific RNA damage to the alpha-sarcin/ricin loop in the 28S rRNA. Mol Cell Biol **17:**3373–3381. http://dx.doi.org/10.1128/MCB.17.6.3373.
17. **Tesh VL.** 2010. Induction of apoptosis by Shiga toxins. Future Microbiol **5:**431–453. http://dx.doi.org/10.2217/fmb.10.4.
18. **Lee SY, Lee MS, Cherla RP, Tesh VL.** 2008. Shiga toxin 1 induces apoptosis through the endoplasmic reticulum stress response in human monocytic cells. Cell Microbiol **10:**770–780. http://dx.doi.org/10.1111/j.1462-5822.2007.01083.x.
19. **Lee MS, Cherla RP, Lentz EK, Leyva-Illades D, Tesh VL.** 2010. Signaling through C/EBP homologous protein and death receptor 5 and calpain activation differentially regulate THP-1 cell maturation-dependent apoptosis induced by Shiga toxin type 1. Infect Immun **78:**3378–3391. http://dx.doi.org/10.1128/IAI.00342-10.
20. **Harrison LM, Cherla RP, van den Hoogen C, van Haaften WC, Lee SY, Tesh VL.** 2005. Comparative evaluation of apoptosis induced by Shiga toxin 1 and/or lipopolysaccharides in human monocytic and macrophage-like cells. Microb Pathog **38:**63–76. http://dx.doi.org/10.1016/j.micpath.2004.12.003.
21. **Lee SY, Cherla RP, Tesh VL.** 2007. Simultaneous induction of apoptotic and survival signaling pathways in macrophage-like THP-1 cells by Shiga toxin 1. Infect Immun **75:**1291–1302. http://dx.doi.org/10.1128/IAI.01700-06.
22. **Lee MS, Kim MH, Tesh VL.** 2013. Shiga toxins expressed by human pathogenic bacteria induce immune responses in host cells. J Microbiol **51:**724–730. http://dx.doi.org/10.1007/s12275-013-3429-6.
23. **Tait Wojno ED, Artis D.** 2012. Innate lymphoid cells: balancing immunity, inflammation, and tissue repair in the intestine. Cell Host Microbe **12:**445–457. http://dx.doi.org/10.1016/j.chom.2012.10.003.
24. **Hurley BP, Jacewicz M, Thorpe CM, Lincicome LL, King AJ, Keusch GT, Acheson DW.** 1999. Shiga toxins 1 and 2 translocate differently across polarized intestinal epithelial cells. Infect Immun **67:**6670–6677.
25. **Sakiri R, Ramegowda B, Tesh VL.** 1998. Shiga toxin type 1 activates tumor necrosis factor-alpha gene transcription and nuclear translocation of the transcriptional activators nuclear factor-kappaB and activator protein-1. Blood **92:**558–566.
26. **Leyva-Illades D, Cherla RP, Galindo CL, Chopra AK, Tesh VL.** 2010. Global transcriptional response of macrophage-like THP-1 cells to Shiga toxin type 1. Infect Immun **78:**2454–2465. http://dx.doi.org/10.1128/IAI.01341-09.
27. **Cherla RP, Lee SY, Mulder RA, Lee MS, Tesh VL.** 2009. Shiga toxin 1-induced proinflammatory cytokine production is regulated by the phosphatidylinositol 3-kinase/Akt/mammalian target of rapamycin signaling pathway. Infect Immun **77:**3919–3931. http://dx.doi.org/10.1128/IAI.00738-09.
28. **Lentz EK, Leyva-Illades D, Lee MS, Cherla RP, Tesh VL.** 2011. Differential response of the human renal proximal tubular epithelial cell line HK-2 to Shiga toxin types 1 and 2. Infect Immun **79:**3527–3540. http://dx.doi.org/10.1128/IAI.05139-11.
29. **Martinon F, Mayor A, Tschopp J.** 2009. The inflammasomes: guardians of the body. Annu Rev Immunol **27:**229–265. http://dx.doi.org/10.1146/annurev.immunol.021908.132715.
30. **Chen G, Shaw MH, Kim YG, Nunez G.** 2009. NOD-like receptors: role in innate immunity and inflammatory disease. Annu Rev Pathol **4:**365–398. http://dx.doi.org/10.1146/annurev.pathol.4.110807.092239.
31. **Lindauer M, Wong J, Magun B.** 2010. Ricin toxin activates the NALP3 inflammasome. Toxins **2:**1500–1514. http://dx.doi.org/10.3390/toxins2061500.
32. **Ohmura M, Yamasaki S, Kurazono H, Kashiwagi K, Igarashi K, Takeda Y.** 1993. Characterization of non-toxic mutant toxins of Vero toxin 1 that were constructed by replacing amino acids in the A subunit. Microb Pathog **15:**169–176. http://dx.doi.org/10.1006/mpat.1993.1067.
33. **Lee MS, Cherla RP, Jenson MH, Leyva-Illades D, Martinez-Moczygemba M, Tesh VL.** 2011. Shiga toxins induce autophagy leading to differential signalling pathways in toxin-sensitive and toxin-resistant

human cells. Cell Microbiol **13:**1479–1496. http://dx.doi.org/10.1111/j.1462-5822.2011.01634.x.
34. **Cory AH, Owen TC, Barltrop JA, Cory JG.** 1991. Use of an aqueous soluble tetrazolium/formazan assay for cell growth assays in culture. Cancer Commun **3:**207–212.
35. **Schroder K, Tschopp J.** 2010. The inflammasomes. Cell **140:**821–832. http://dx.doi.org/10.1016/j.cell.2010.01.040.
36. **Franchi L, Munoz-Planillo R, Nunez G.** 2012. Sensing and reacting to microbes through the inflammasomes. Nat Immunol **13:**325–332. http://dx.doi.org/10.1038/ni.2231.
37. **Latz E, Xiao TS, Stutz A.** 2013. Activation and regulation of the inflammasomes. Nat Rev Immunol **13:**397–411. http://dx.doi.org/10.1038/nri3452.
38. **Vyleta ML, Wong J, Magun BE.** 2012. Suppression of ribosomal function triggers innate immune signaling through activation of the NLRP3 inflammasome. PLoS One **7:**e36044. http://dx.doi.org/10.1371/journal.pone.0036044.
39. **Miao EA, Rajan JV, Aderem A.** 2011. Caspase-1-induced pyroptotic cell death. Immunol Rev **243:**206–214. http://dx.doi.org/10.1111/j.1600-065X.2011.01044.x.
40. **Dinarello CA.** 2009. Immunological and inflammatory functions of the interleukin-1 family. Annu Rev Immunol **27:**519–550. http://dx.doi.org/10.1146/annurev.immunol.021908.132612.
41. **Harrison LM, van den Hoogen C, van Haaften WC, Tesh VL.** 2005. Chemokine expression in the monocytic cell line THP-1 in response to purified Shiga toxin 1 and/or lipopolysaccharides. Infect Immun **73:**403–412. http://dx.doi.org/10.1128/IAI.73.1.403-412.2005.
42. **Leyva-Illades D, Cherla RP, Lee MS, Tesh VL.** 2012. Regulation of cytokine and chemokine expression by the ribotoxic stress response elicited by Shiga toxin type 1 in human macrophage-like THP-1 cells. Infect Immun **80:**2109–2120. http://dx.doi.org/10.1128/IAI.06025-11.
43. **Nunes-Alves C.** 2014. Inflammasomes: new LPS receptors discovered. Nat Rev Immunol **14:**582.
44. **Shi J, Zhao Y, Wang Y, Gao W, Ding J, Li P, Hu L, Shao F.** 2014. Inflammatory caspases are innate immune receptors for intracellular LPS. Nature **514:**187–192.
45. **Keepers TR, Psotka MA, Gross LK, Obrig TG.** 2006. A murine model of HUS: Shiga toxin with lipopolysaccharide mimics the renal damage and physiologic response of human disease. J Am Soc Nephrol **17:**3404–3414. http://dx.doi.org/10.1681/ASN.2006050419.
46. **Fernandes-Alnemri T, Alnemri ES.** 2008. Assembly, purification, and assay of the activity of the ASC pyroptosome. Methods Enzymol **442:**251–270. http://dx.doi.org/10.1016/S0076-6879(08)01413-4.
47. **Fernandes-Alnemri T, Wu J, Yu JW, Datta P, Miller B, Jankowski W, Rosenberg S, Zhang J, Alnemri ES.** 2007. The pyroptosome: a supramolecular assembly of ASC dimers mediating inflammatory cell death via caspase-1 activation. Cell Death Differ **14:**1590–1604. http://dx.doi.org/10.1038/sj.cdd.4402194.
48. **Tesh VL.** 2012. Activation of cell stress response pathways by Shiga toxins. Cell Microbiol **14:**1–9. http://dx.doi.org/10.1111/j.1462-5822.2011.01684.x.
49. **Raa H, Grimmer S, Schwudke D, Bergan J, Walchli S, Skotland T, Shevchenko A, Sandvig K.** 2009. Glycosphingolipid requirements for endosome-to-Golgi transport of Shiga toxin. Traffic **10:**868–882. http://dx.doi.org/10.1111/j.1600-0854.2009.00919.x.
50. **Lee HM, Kim JJ, Kim HJ, Shong M, Ku BJ, Jo EK.** 2013. Upregulated NLRP3 inflammasome activation in patients with type 2 diabetes. Diabetes **62:**194–204. http://dx.doi.org/10.2337/db12-0420.
51. **Lu A, Magupalli VG, Ruan J, Yin Q, Atianand MK, Vos MR, Schroder GF, Fitzgerald KA, Wu H, Egelman EH.** 2014. Unified polymerization mechanism for the assembly of ASC-dependent inflammasomes. Cell **156:**1193–1206. http://dx.doi.org/10.1016/j.cell.2014.02.008.
52. **Sagulenko V, Thygesen SJ, Sester DP, Idris A, Cridland JA, Vajjhala PR, Roberts TL, Schroder K, Vince JE, Hill JM, Silke J, Stacey KJ.** 2013. AIM2 and NLRP3 inflammasomes activate both apoptotic and pyroptotic death pathways via ASC. Cell Death Differ **20:**1149–1160. http://dx.doi.org/10.1038/cdd.2013.37.
53. **Feldmann M.** 2002. Development of anti-TNF therapy for rheumatoid arthritis. Nat Rev Immunol **2:**364–371. http://dx.doi.org/10.1038/nri802.
54. **Lin WJ, Yeh WC.** 2005. Implication of Toll-like receptor and tumor necrosis factor alpha signaling in septic shock. Shock **24:**206–209. http://dx.doi.org/10.1097/01.shk.0000180074.69143.77.
55. **van de Kar NC, Monnens LA, Karmali MA, van Hinsbergh VW.** 1992. Tumor necrosis factor and interleukin-1 induce expression of the verocytotoxin receptor globotriaosylceramide on human endothelial cells: implications for the pathogenesis of the hemolytic uremic syndrome. Blood **80:**2755–2764.
56. **Cherla RP, Lee SY, Mees PL, Tesh VL.** 2006. Shiga toxin 1-induced cytokine production is mediated by MAP kinase pathways and translation initiation factor eIF4E in the macrophage-like THP-1 cell line. J Leukoc Biol **79:**397–407.
57. **Jacewicz MS, Mobassaleh M, Gross SK, Balasubramanian KA, Daniel PF, Raghavan S, McCluer RH, Keusch GT.** 1994. Pathogenesis of Shigella diarrhea: XVII. A mammalian cell membrane glycolipid, Gb3, is required but not sufficient to confer sensitivity to Shiga toxin. J Infect Dis **169:**538–546.
58. **Zumbrun SD, Hanson L, Sinclair JF, Freedy J, Melton-Celsa AR, Rodriguez-Canales J, Hanson JC, O'Brien AD.** 2010. Human intestinal tissue and cultured colonic cells contain globotriaosylceramide synthase mRNA and the alternate Shiga toxin receptor globotetraosylceramide. Infect Immun **78:**4488–4499. http://dx.doi.org/10.1128/IAI.00620-10.
59. **Lee MS, Cherla RP, Tesh VL.** 2010. Shiga toxins: intracellular trafficking to the ER leading to activation of host cell stress responses. Toxins **2:**1515–1535. http://dx.doi.org/10.3390/toxins2061515.
60. **Jones NL, Islur A, Haq R, Mascarenhas M, Karmali MA, Perdue MH, Zanke BW, Sherman PM.** 2000. Escherichia coli Shiga toxins induce apoptosis in epithelial cells that is regulated by the Bcl-2 family. Am J Physiol Gastrointest Liver Physiol **278:**G811–G819.
61. **Baibakov B, Murtazina R, Elowsky C, Giardiello FM, Kovbasnjuk O.** 2010. Shiga toxin is transported into the nucleoli of intestinal epithelial cells via a carrier-dependent process. Toxins **2:**1318–1335. http://dx.doi.org/10.3390/toxins2061318.
62. **Harrison LM, van Haaften WC, Tesh VL.** 2004. Regulation of proinflammatory cytokine expression by Shiga toxin 1 and/or lipopolysaccharides in the human monocytic cell line THP-1. Infect Immun **72:**2618–2627. http://dx.doi.org/10.1128/IAI.72.5.2618-2627.2004.
63. **Mariathasan S, Weiss DS, Newton K, McBride J, O'Rourke K, Roose-Girma M, Lee WP, Weinrauch Y, Monack DM, Dixit VM.** 2006. Cryopyrin activates the inflammasome in response to toxins and ATP. Nature **440:**228–232. http://dx.doi.org/10.1038/nature04515.
64. **McCoy AJ, Koizumi Y, Higa N, Suzuki T.** 2010. Differential regulation of caspase-1 activation via NLRP3/NLRC4 inflammasomes mediated by aerolysin and type III secretion system during Aeromonas veronii infection. J Immunol **185:**7077–7084. http://dx.doi.org/10.4049/jimmunol.1002165.
65. **McCoy AJ, Koizumi Y, Toma C, Higa N, Dixit V, Taniguchi S, Tschopp J, Suzuki T.** 2010. Cytotoxins of the human pathogen Aeromonas hydrophila trigger, via the NLRP3 inflammasome, caspase-1 activation in macrophages. Eur J Immunol **40:**2797–2803. http://dx.doi.org/10.1002/eji.201040490.
66. **Koizumi Y, Toma C, Higa N, Nohara T, Nakasone N, Suzuki T.** 2012. Inflammasome activation via intracellular NLRs triggered by bacterial infection. Cell Microbiol **14:**149–154. http://dx.doi.org/10.1111/j.1462-5822.2011.01707.x.
67. **Bauernfeind FG, Horvath G, Stutz A, Alnemri ES, MacDonald K, Speert D, Fernandes-Alnemri T, Wu J, Monks BG, Fitzgerald KA, Hornung V, Latz E.** 2009. Cutting edge: NF-kappaB activating pattern recognition and cytokine receptors license NLRP3 inflammasome activation by regulating NLRP3 expression. J Immunol **183:**787–791. http://dx.doi.org/10.4049/jimmunol.0901363.
68. **Ishii H, Takada K, Higuchi T, Sugiyama J.** 2000. Verotoxin-1 induces tissue factor expression in human umbilical vein endothelial cells through activation of NF-kappaB/Rel and AP-1. Thromb Haemost **84:**712–721.
69. **Manning SD, Motiwala AS, Springman AC, Qi W, Lacher DW, Ouellette LM, Mladonicky JM, Somsel P, Rudrik JT, Dietrich SE, Zhang W, Swaminathan B, Alland D, Whittam TS.** 2008. Variation in virulence among clades of Escherichia coli O157:H7 associated with disease outbreaks. Proc Natl Acad Sci U S A **105:**4868–4873. http://dx.doi.org/10.1073/pnas.0710834105.
70. **Stearns-Kurosawa DJ, Collins V, Freeman S, Tesh VL, Kurosawa S.** 2010. Distinct physiologic and inflammatory responses elicited in baboons after challenge with Shiga toxin type 1 or 2 from enterohemorrhagic Escherichia coli. Infect Immun **78:**2497–2504. http://dx.doi.org/10.1128/IAI.01435-09.
71. **Pierini R, Juruj C, Perret M, Jones CL, Mangeot P, Weiss DS, Henry T.** 2012. AIM2/ASC triggers caspase-8-dependent apoptosis in Francisella-

infected caspase-1-deficient macrophages. Cell Death Differ **19:**1709–1721. http://dx.doi.org/10.1038/cdd.2012.51.

72. **Abdelaziz DH, Gavrilin MA, Akhter A, Caution K, Kotrange S, Khweek AA, Abdulrahman BA, Hassan ZA, El-Sharkawi FZ, Bedi SS, Ladner K, Gonzalez-Mejia ME, Doseff AI, Mostafa M, Kanneganti TD, Guttridge D, Marsh CB, Wewers MD, Amer AO.** 2011. Asc-dependent and independent mechanisms contribute to restriction of legionella pneumophila infection in murine macrophages. Front Microbiol **2:**18.
73. **Smith WE, Kane AV, Campbell ST, Acheson DW, Cochran BH, Thorpe CM.** 2003. Shiga toxin 1 triggers a ribotoxic stress response leading to p38 and JNK activation and induction of apoptosis in intestinal epithelial cells. Infect Immun **71:**1497–1504. http://dx.doi.org/10.1128/IAI.71.3.1497-1504.2003.
74. **Kailasan Vanaja S, Rathinam VA, Atianand MK, Kalantari P, Skehan B, Fitzgerald KA, Leong JM.** 2014. Bacterial RNA:DNA hybrids are activators of the NLRP3 inflammasome. Proc Natl Acad Sci U S A **111:**7765–7770. http://dx.doi.org/10.1073/pnas.1400075111.